Energy Levels in $V^{47,49,51}$ and $Mn^{51,53,55}$ from (He^3, d) Reactions

B. ČUJEC AND I. M. SZÖGHY
Université Laval, Québec, Canada

(Received 15 July 1968)

The $Ti^{46,48,50}$(He^3, d)$V^{47,49,51}$ and $Cr^{50,52,54}$(He^3, d)$Mn^{51,53,55}$ reactions are studied with high resolution at 10- and 9.5-MeV incident energies, respectively. The l values and spectroscopic factors are extracted by means of the distorted-wave Born-approximation calculations. A systematic study of the $p_{3/2}$ centroid energies, of the $d_{3/2}$ and $s_{1/2}$ proton hole states, and of the splitting of the $p_{3/2}$ spectroscopic strength is presented. These quantities, and also the individual energy spectra, are compared with the expectations of the shell model and the Coriolis strong-coupling model. It is concluded that the shell model adequately describes these nuclei, while the Coriolis strong-coupling model fails to explain the observed splitting of the $p_{3/2}$ spectroscopic strength.

INTRODUCTION

This work started with the intention to study systematically the single-particle proton states in the $f_{7/2}$ shell nuclei by means of the (He^3, d) reactions on even-even targets. As the reactions $Ca^{42,44,46,48}$ (He^3, d) $Sc^{43,45,47,49}$ had already been studied[1,2] in other laboratories, and the results[3] on the $Fe^{54,56}$ (He^3, d) $Co^{55,57}$ reactions became known to us at an early stage, we limited ourselves to the $Ti^{46,48,50}$ (He^3, d) $V^{47,49,51}$ and $Cr^{50,52,54}$ (He^3, d) $Mn^{51,53,55}$ reactions.[4] Also here we did not remain alone. MIT studied[5-7] V^{47}, V^{51}, Mn^{51}, and Mn^{53} at 12, 10, 12, and 11 MeV, respectively, University of Pennsylvania[8,9] V^{47} and V^{49} at 16.5 and 17 MeV, and Heidelberg[10] V^{49} at 18 MeV. Only the Cr^{54} (He^3, d) Mn^{55} reaction remains unique to our work. Nevertheless, we believe that the presentation of our data in a complete form is useful. It gives additional information about l values and spectroscopic factors and contributes to our knowledge of the DWBA method and the consistency of spectroscopic factors extracted at different incident energies. The advantage of the present study is that the spectroscopic factors were obtained for all six isotopes under the same experimental conditions and by using the same optical model parameters and normalization constant.

TABLE I. Experimental conditions.

Target	Enrichment (%)	Q value (MeV)	Incident energy (MeV)	Elastic scattering $d\sigma/d\Omega$(92.5°) (mb/sr)
Ti^{46}	84.5	−0.301	10	34.9
Ti^{48}	99.1	1.259	9, 10	53.0, 34.9
Ti^{50}	69.7	2.552	10	34.9
Cr^{50}	95	−0.206	9.5	59.5
Cr^{52}	99	1.070	9.5	65.5
Cr^{54}	94	2.565	8, 9.5	124.5, 65.0

EXPERIMENTAL PROCEDURE

Measurements were carried out using the facilities of the 5.5-MV Van de Graaff accelerator at Laval University, giving a beam of doubly charged He^3 ions up to 11 MeV. The outgoing deuterons were analyzed by a broad-range magnetic spectrograph and detected with photographic plates. The deuterons up to the maximum energy of 10 MeV were focused along a plate 25-cm long, placed at 30° with respect to the incident particles. With one exposure, the levels within an energy interval of about 1.7 MeV were obtained.

The targets were prepared from enriched isotopes (Table I) by evaporation on 200-$\mu g/cm^2$-thick gold foil. The thickness of the targets ranged between 70 $\mu g/cm^2$ (measurements of 25-keV resolution) and 500 $\mu g/cm^2$ (measurements of 85-keV resolution). The beam current on the target varied between 0.1 and 0.2 μA. The incident energy was, as a rule, 10 MeV for titanium and 9.5 MeV for chromium isotopes. In cases where the deuterons were of too high an energy to be bent, the lower part of the spectrum was investigated with a lower bombarding energy (Table I). No particular effort was made to study the V^{51} levels below 2.4 MeV, because the spectrum was already well known[11] and in a few exposures with 8-MeV incident energy only the ground state was seen.

[1] J. J. Schwartz and W. Parker Alford, Phys. Rev. **149**, 820 (1966); J. J. Schwartz, W. Parker Alford, and A. Marinov, *ibid.* **153**, 1248 (1966).
[2] J. R. Erskine, A. Marinov, and J. P. Schiffer, Phys. Rev. **142**, 633 (1965).
[3] B. Rosner and C. H. Holbrow, Phys. Rev. **154**, 1080 (1967).
[4] Preliminary results have been reported at C.A.P. Congress, 1966; Physics in Canada **22**, No. 2, 60 (1966).
[5] W. E. Dorenbusch, J. Rapaport, and T. A. Belote, Nucl. Phys. **A102**, 681 (1967).
[6] B. J. O'Brien, W. E. Dorenbusch, T. A. Belote, and J. Rapaport, Nucl. Phys. **A104**, 609 (1967).
[7] J. Rapaport, T. A. Belote, and W. E. Dorenbusch, Nucl. Phys. **A100**, 280 (1967).
[8] B. Rosner and D. J. Pullen, Phys. Rev. **162**, 1048 (1967).
[9] D. J. Pullen, Baruch Rosner, and Ole Hansen, Phys. Rev. **166**, 1142 (1968).
[10] D. Bachner, R. Santo, H. H. Duhm, R. Bock, and S. Hinds, Nucl. Phys. **A106**, 577 (1968).
[11] *Nuclear Data Sheets*, compiled by K. Way *et al.* (U.S. Government Printing Office, National Academy of Sciences–National Research Council, Washington, D.C. 20025, 1960).

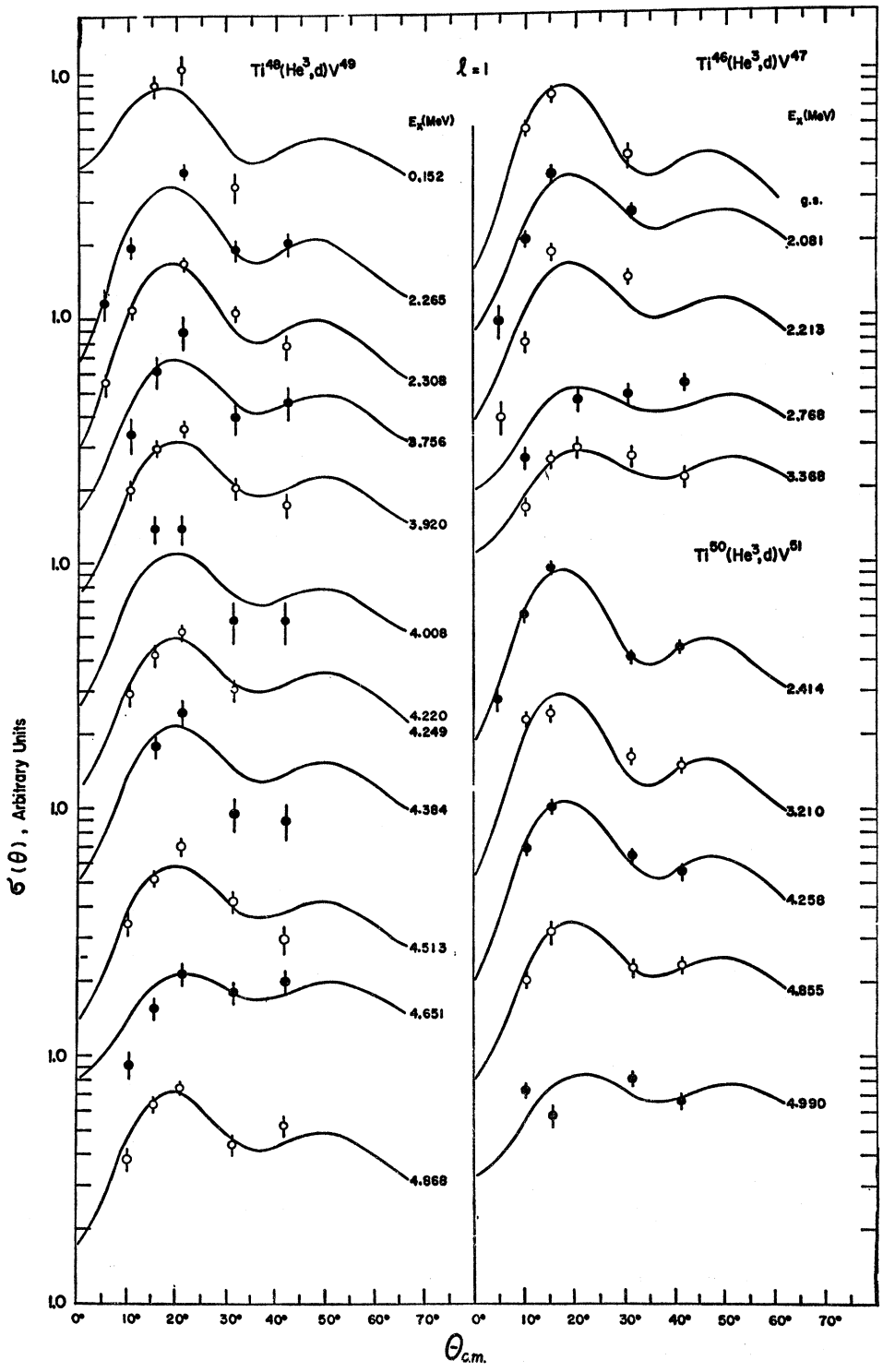

FIG. 1. $l=1$ angular distributions observed with $Ti^{46,48,50}(He^3, d)V^{47,49,51}$ reactions. The incident energy is 10 MeV. The curves represent DWBA calculations.

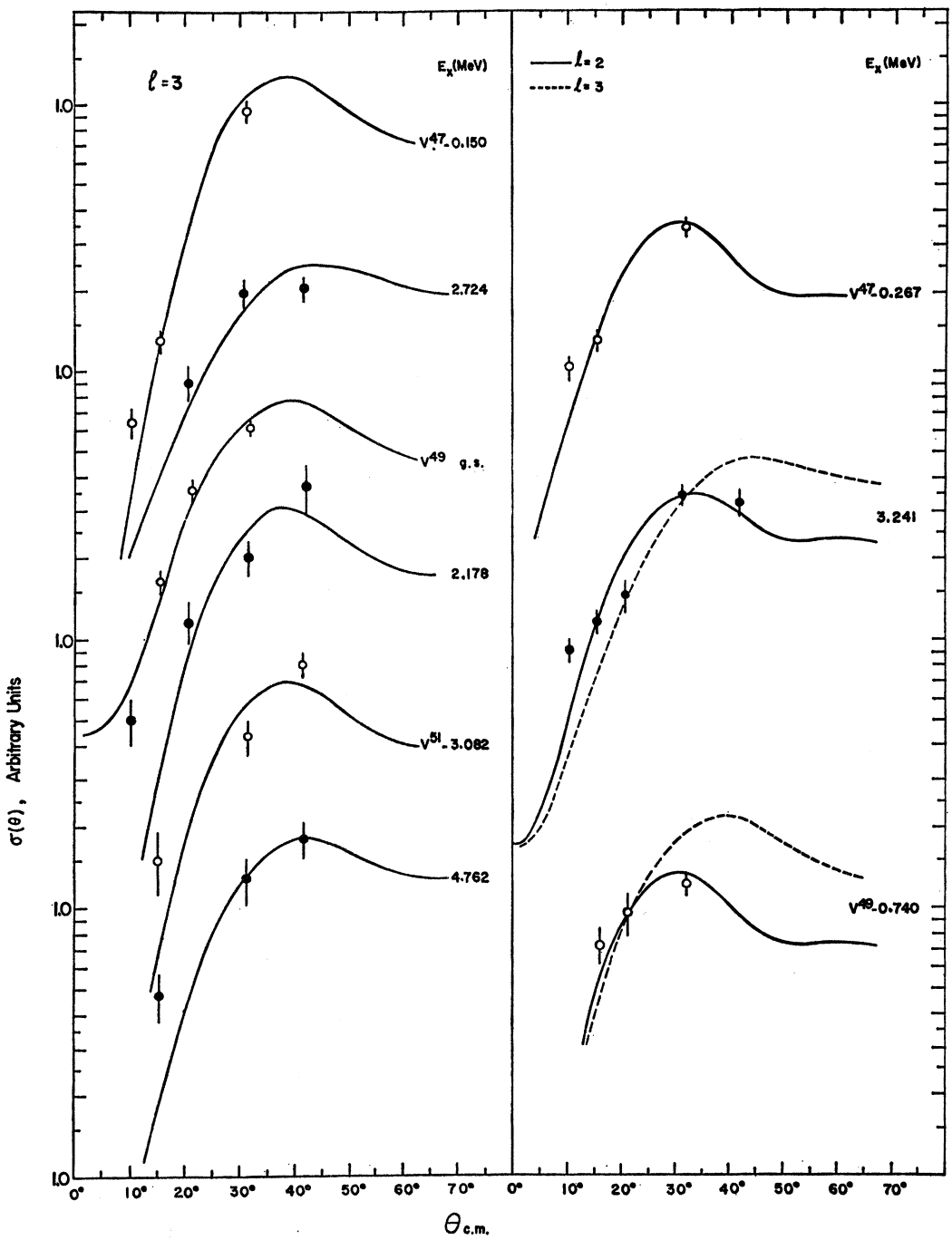

FIG. 2. $l=3$ and $l=2$ angular distributions observed with $Ti^{46,48,50}(He^3, d)V^{47,49,51}$ reactions. The incident energy is 10 MeV. The curves represent DWBA calculations.

Measurements were obtained at laboratory angles of 10°, 20°, 30°, 40°, and also, in some cases, at 5°, 90°, and 135°. Kodak NTB plates, 100 μ thick, were covered with aluminium foil, which stopped He^3 and α particles and reduced deuterons to about half of the maximum range available in the emulsion, so that deuterons were easily distinguishable from protons by track length.

Absolute cross sections were obtained by measuring the yield of the elastically scattered He^3 particles at 92.5° (laboratory angle), and from the measured elastic scattering cross sections at this angle. These

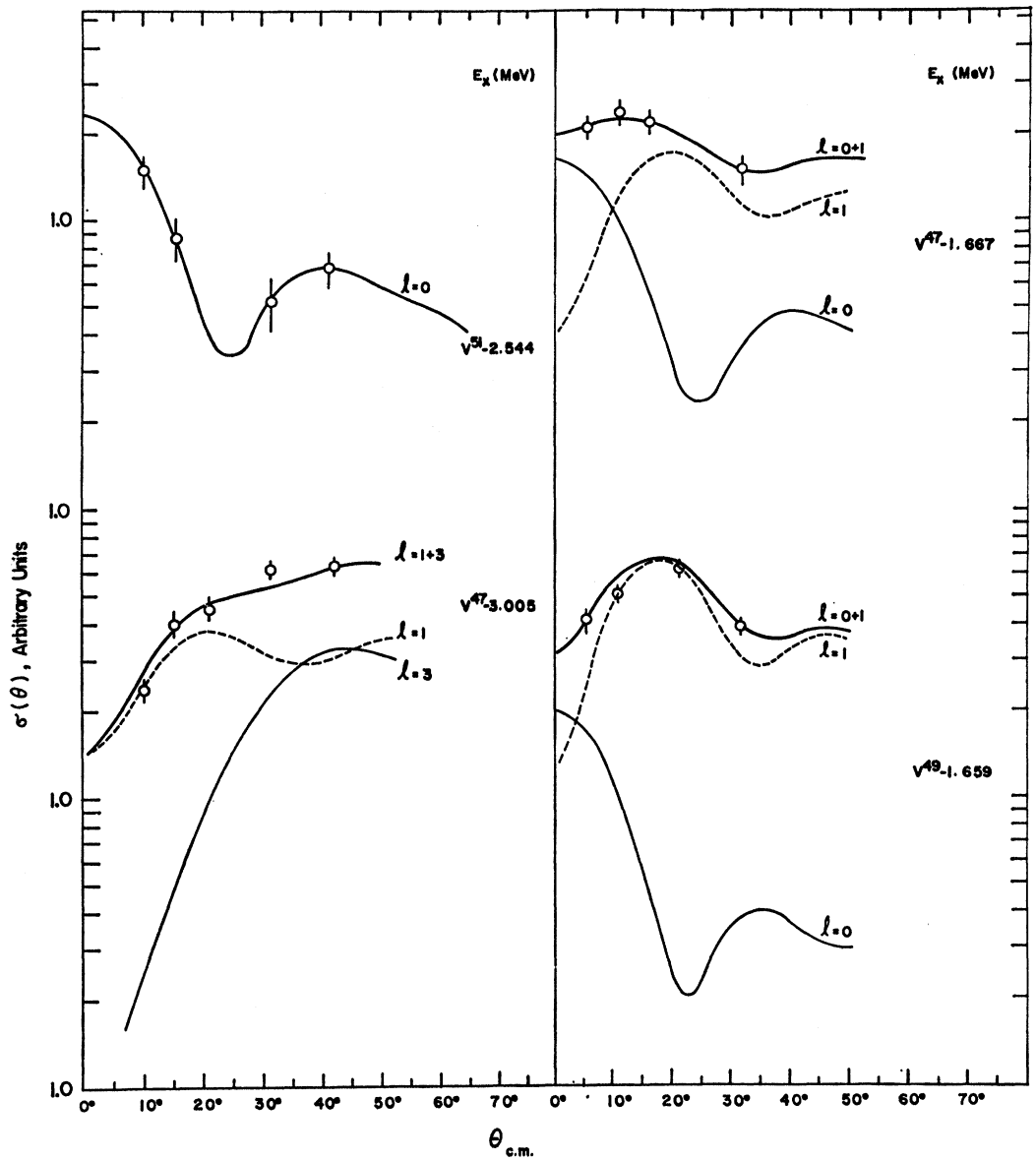

FIG. 3. (He^3, d) angular distributions leading to the V^{51}, 2.544-MeV level and to the levels interpreted as doublets: V^{47}, 1.667 MeV; V^{47}, 3.005 MeV; and V^{49}, 1.659 MeV. The incident energy is 10 MeV. The curves represent DWBA calculations. For the doublets the curve through experimental points is the sum of two curves with given l values.

elastic scattering cross sections are listed in Table I, and were obtained by measuring the angular distribution, and by assuming, at 8-MeV incident energy with angles smaller than 30°, that the Rutherford approximation is adequate. The accuracy in the (He^3, d) absolute cross sections is 20%.

ANALYSIS AND RESULTS

Excitation energies were calculated from the position of observed peaks by a computer program, using a carefully obtained relationship between the position on the plate and the $B\rho Z$ value. Peaks due to contaminants were eliminated by observing the dependence of the particle energy on the scattering angle. The agreement with other[11–15] high-resolution data is within 10 keV.

The experimental and calculated angular distributions are shown in Figs. 1–7. The DWBA calculations

[12] G. Brown, A. MacGregor, R. Middleton, Nucl. Phys. **77**, 385 (1966).
[13] H. Albinsson and J. Dubois, Phys. Letters **15**, 260 (1960).
[14] G. Brown, S. E. Warren, and R. Middleton, Nucl. Phys. **77**, 365 (1966).
[15] N. Wall and B. Erlandsson, Arkiv Fysik **34**, 325 (1967).

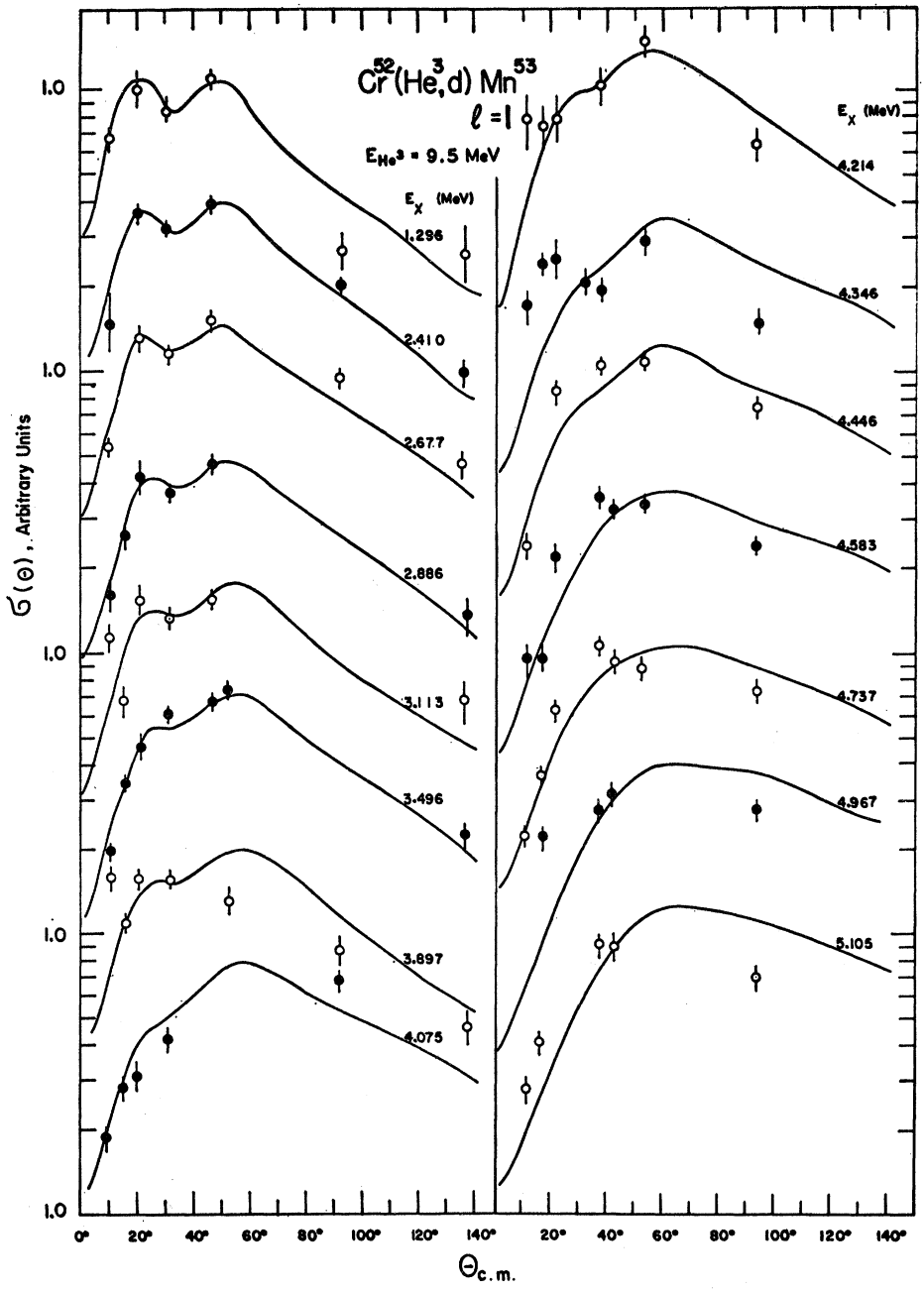

FIG. 4. $l=1$ angular distributions observed with $Cr^{52}(He^3, d)Mn^{53}$. The incident energy is 9.5 MeV. The curves represent DWBA calculations.

were performed with the computer code T-SALLY.[16] The optical-model parameters used in this analysis are listed in Table II. That they fit the observed angular distributions was also demonstrated by St.-Pierre *et al.*[17] of this laboratory, who measured complete angular distributions from 20°–120° for strongly excited peaks of V^{47}, V^{49}, and V^{51} by means of a semiconductor $E-\Delta E$ detector. The shape of the calculated angular distribution and the value of the cross section depend rather sensitively on the Z value of the target and on the incident energy. This is not surprising, since the incident energy is close to the height of the Coulomb barrier (~9 MeV). Nevertheless, the transitions with different l values remain clearly distinguishable. The

[16] R. H. Bassel, R. M. Drisko and G. R. Satchler, Oak Ridge National Laboratory Report No. ORNL-3240, 1962 (unpublished); and (private communication).

[17] C. St.-Pierre, P. N. Maheshwari, D. Doutriaux, and L. Lamarche, Nucl. Phys. A102, 433 (1967).

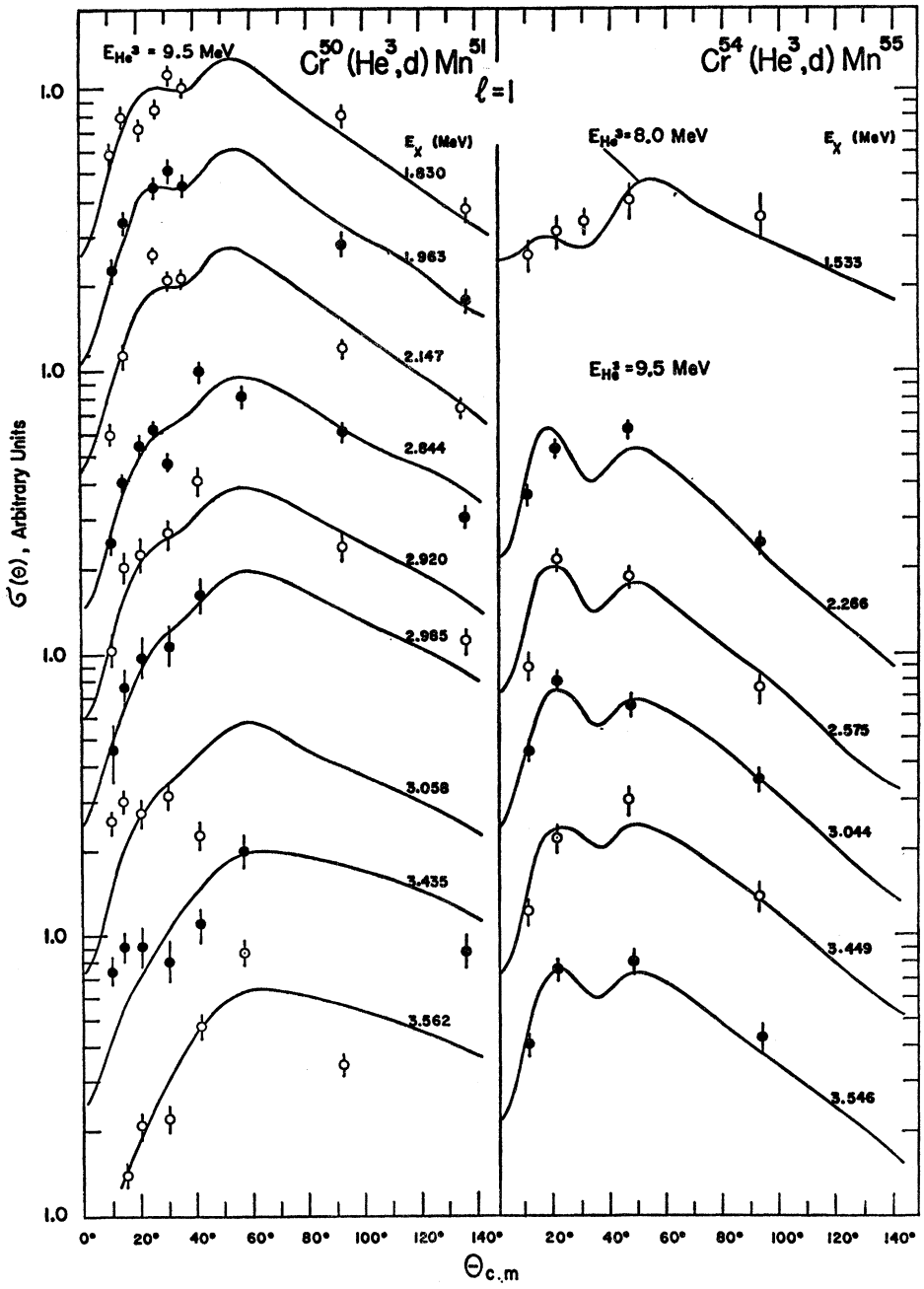

FIG. 5. $l=1$ angular distributions observed with $Cr^{50}(He^3, d)$ Mn^{51} and $Cr^{54}(He^3, d)Mn^{55}$. The incident energy is 9.5 MeV, except for the Mn^{55} 1.533-MeV level, where it is 8 MeV. The curves represent DWBA calculations.

calculations without cutoff were used; those with a cutoff (4 and 6 F) gave almost identical results. We also tried two additional sets of optical-model parameters: the deuteron parameters[18] derived from Ti at 11.8 MeV, and the He^3 parameters[19] derived from Ti^{48} at 12 MeV, neither of which fitted the observed angular distributions.

[18] C. M. Perey and F. G. Perey, Phys. Rev. **132**, 755 (1963).
[19] J. L. Yntema, B. Zeidman, and R. H. Bassel, Phys. Letters **11**, 302 (1964).

The spectroscopic strength $(2J+1)C^2S$ is obtained from the relation

$$d\sigma/d\Omega = N(2J+1)C^2S\sigma_{\mathrm{DWBA}},$$

where σ_{DWBA} is the calculated cross section, $d\sigma/d\Omega$ is the measured cross section, and N is a normalization constant. Following the suggestion by Satchler,[2] the cross sections calculated by the code T-SALLY were corrected for the slight j dependence: The calculated $l=1$ cross section was multiplied by 1.06 for $\frac{3}{2}^-$ state and

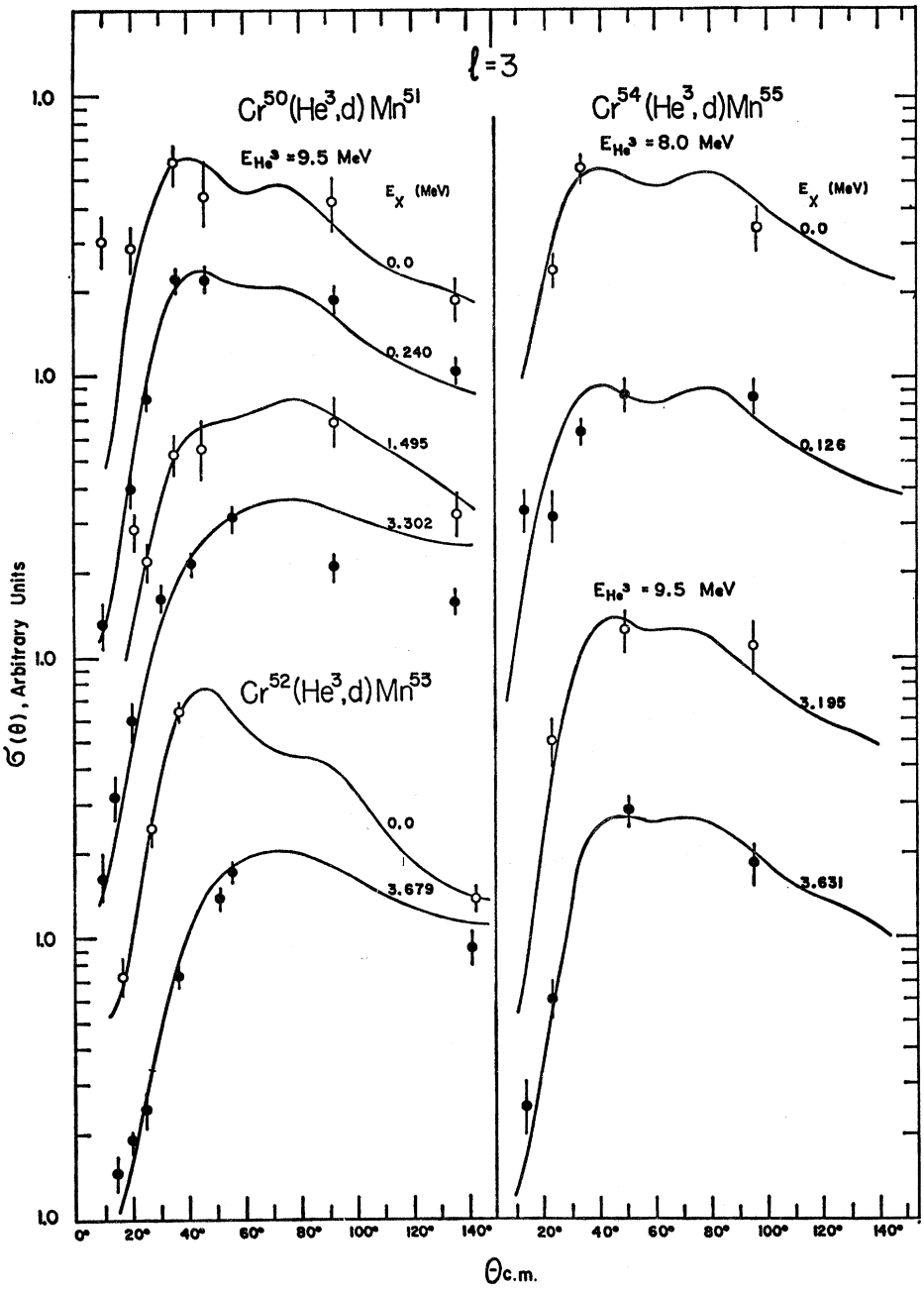

FIG. 6. $l=3$ angular distributions observed with $Cr^{50,52,54}(He^3, d)Mn^{51,53,55}$ reactions. The incident energies are 8 and 9.5 MeV. The curves represent DWBA calculations.

by 0.94 for a $\frac{1}{2}^-$ state, and the calculated $l=3$ cross section was multiplied by 1.2 for a $\frac{7}{2}^-$ state and by 0.8 for a $\frac{5}{2}^-$ state. The j value assumed in correction was the one listed first in the column J^π of Table III. The two possible spectroscopic strengths differ by 12% in the $l=1$ case and by 40% in the $l=3$ case, the value being larger for $j=l-\frac{1}{2}$ than for $j=l+\frac{1}{2}$.

We have chosen to determine the constant N by a normalization procedure based on the total $f_{7/2}T_<$ strength rather than to adopt the value 4.42, calculated[20] from wave functions for He^3 and the deuteron. It was assumed that the $f_{7/2}T_<$ strength is exhausted by the transitions to the levels listed in the third column of Table IV. For V^{47}, V^{51}, Mn^{53}, and Mn^{55}, the levels in question are just the ground state or the first excited state. For V^{49} and Mn^{51}, one more level is

[20] R. H. Bassel, Phys. Rev. 149, 791 (1966).

TABLE II. Optical-model parameters.[a]

Particle	V (MeV)	r_0 (F)	a (F)	W (MeV)	W' (MeV)	r' (F)	a' (F)	r_c (F)
He^3 [b]	174.5	1.07	0.85	13.5	...	1.81	0.59	1.4
Deuteron[c]	112	1.0	0.9	...	72	1.55	0.47	1.3
Bound state[d]	B_p	1.25	0.65	...	...	...	...	1.25

[a] The potentials are of the form: $U(r) = -V(e^x+1)^{-1} - i(W-W'\, d/dx')(e^{x'}+1)^{-1} + U_c(r)$, with, $x=(r-r_0A^{1/3})/a$ and $x'=(r-r_0'A^{1/3})/a'$.

[b] Parameters derived from Ca^{40} by D. Cline *et al.*, Nucl. Phys. **73**, 33 (1965).

[c] Parameters derived from Ca^{40} by R. H. Bassel *et al.*, Phys. Rev. **136**, 960 (1964).

[d] Adjustment so that the proton gets a binding energy $B_p = Q + 5.49$ MeV.

included, for V^{49}, the level at 2.18 MeV contributing 17%, and for Mn^{51}, the level at 1.50 MeV contributing 6% to the total $f_{7/2}T_<$ strength. The concentration of the $f_{7/2}T_<$ in just one level is theoretically predicted and experimentally confirmed. Shell-model calculations[21,22] concentrate all or almost all (90%) of the $f_{7/2}T_<$ spectroscopic strength in the ground state or a nearly level. Experimentally, all other $l=3$ transitions observed with appreciable strength are about 3 MeV higher in energy. This concentration of the $f_{7/2}T_<$ strength makes the normalization procedure easy and reliable.

In that way the mean value $N=2.5$ with the sample standard deviation 0.2 was obtained. In order to account for eventual admixtures in the target ground-state wave function, we increased N to 2.6. Allowing for an error of 20% in experimental cross section and of 15% in σ_{DWBA}, we estimate the error in N to 25%. The value $N=2.6\pm0.7$ so obtained is essentially smaller than the calculated[20] value $N=4.42$ or $N=3.84$. The difference with $N=4.42$ remains significant (the level of significance = 0.05) even if one allows for 20% admixture in intensity (45% in amplitude) of other than $f_{7/2}^n$ components in the target ground-state wave function. Our constant, however, is not significantly different from the value $N=3.48$ obtained[2] by a similar procedure for Ca^{48} (He^3, d) Sc^{49} reaction, and agrees with the constant found in the (d, He^3) work.[23,24] These two constants are simply related by the statistical factor, depending on the spins of the deuteron and He^3, by $N(He^3, d) = \frac{3}{2}N(d, He^3)$. Accordingly, $N(d, He^3) = 1.73$ corresponds to $N(He^3, d) = 2.6$. The former is to be compared with values 1.5 (Ref. 23) and 1.6, 1.9 (Ref. 24) obtained in (d, He^3) work.

With our choice of N the $p_{3/2}T_<$ strengths are exhausted up to an excitation energy between 3.4 and 4.9 MeV, and the $p_{3/2}T_<$ centroid energies have very reasonable values [see Table IV and the text following Eq. (3)]. On the other hand, the application of $N=4.42$ in connection with σ_{DWBA} calculated with the optical-model parameters which are similar to ours gives too small sums for the $l=1$ spectroscopic strengths. For $Ca^{46}(He^3, d)Sc^{47}$ Schwartz *et al.*[1] concluded that they observed only about 60% of the $p_{3/2}T_<$ and of the $p_{1/2}T_<$ strength (up to 7.5-MeV excitation). Similarly, about 60% of the $l=1$, $T_<$ strength is observed by MIT[5-7] up to about 6-MeV excitation. This percentage is not higher in the Pennsylvania work[9] where the measurements reach as high as 8.6 MeV in excitation. This deficiency is removed if the constant 4.42 which they used is replaced by $N=2.6$, the ratio of the two constants being 0.59.

The results concerning levels observed with the (He^3, d) reactions are presented in Table III. From other reactions and γ-ray transitions many more levels are known[11-15] to exist and they are shown in Figs.

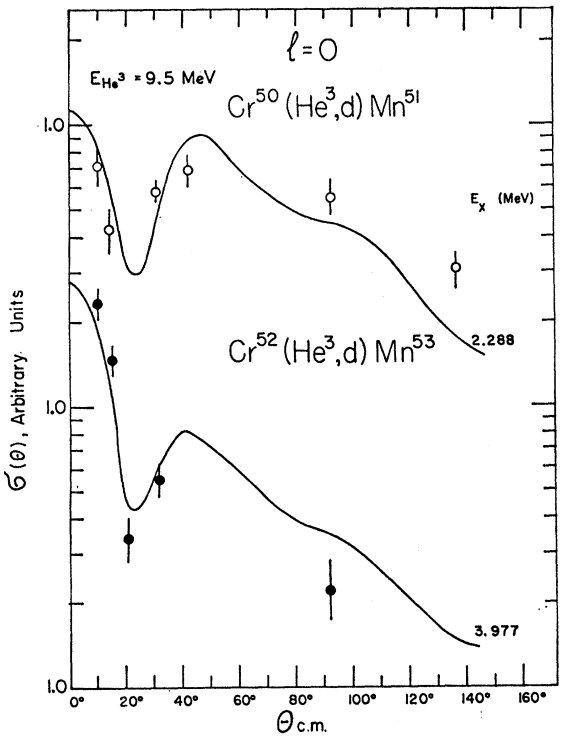

FIG. 7. $l=0$ angular distributions for Mn^{51} 2.228-MeV level and Mn^{53} 3.997-MeV level. The incident energy is 9.5 MeV. The curves represent DWBA calculations.

[21] J. D. McCullen, B. F. Bayman, and L. Zamick, Phys. Rev. **134**, B515 (1964).
[22] J. N. Ginocchio, Phys. Rev. **144**, 952 (1965).
[23] B. Čujec, Phys. Rev. **128**, 2303 (1962).
[24] J. L. Yntema and G. R. Satchler, Phys. Rev. **134**, B976 (1964).

TABLE III. Summary of experimental results.

Excitation[a] energy (MeV)	Peak[b] cross section (mb/sr)	l	J^π	Spectroscopic strength $(2J+1)C^2S$ This work[c]		Other work	
$Ti^{46}(He^3, d)V^{47}$				$E_{He^3}=10$ MeV	10 MeV[d]	12 MeV[e]	16.6 MeV[f]
0	0.30	1	$\frac{3}{2}^-$ [g]	0.16	0.12	0.11	0.16
0.089	0.08		$\frac{5}{2}^-$ [h]				
0.150	1.00	3	$\frac{7}{2}^-$ [i]	4.85	3.92	2.83	4.64
0.267	0.27	2	$\frac{3}{2}^+$ [j]	(0.78)		0.46	0.32
0.670	0.14						
1.667	0.32	1	$\frac{3}{2}^-, \frac{1}{2}^-$	0.13	0.08	0.09	0.12
	0.30	0[e,f] 0	$\frac{1}{2}^+$	0.07			
2.081	3.40	1	$\frac{3}{2}^-$[k]	1.49	1.04	0.76	1.40
2.213	1.54	1	$\frac{3}{2}^-, \frac{1}{2}^-$	0.66	0.56	0.37	0.60
2.544	0.30	3	$\frac{5}{2}^-, \frac{7}{2}^-$	1.62		0.74	1.38
2.724	0.13	3, 2[e], 3[f]	$\frac{5}{2}^-, \frac{7}{2}^-$	0.70		0.18	0.96
2.768	0.18	1	$\frac{3}{2}^-, \frac{1}{2}^-$	0.07		0.06	0.28
3.005[l]	0.30	1	$\frac{3}{2}^-, \frac{1}{2}^-$	0.12		0.09	0.12
	0.25	1[e,f] 3	$\frac{5}{2}^-, \frac{7}{2}^-$	1.31			
3.241	0.21, 0.29	2, 3	$(\frac{3}{2}^+, \frac{5}{2}^-)$	(0.16, 1.55)			
3.368	0.26	1	$\frac{3}{2}^-, \frac{1}{2}^-$	0.11		0.08	0.14
$Ti^{48}(He^3, d)V^{49}$				$E_{He^3}=9$ MeV	10 MeV[d]	17 MeV[m]	18 MeV[n]
0	0.52	3	$\frac{7}{2}^-$ [o]	4.90	4.64	2.50	4.30
0.091	0.02		$(\frac{5}{2})^-$ [o]				
0.152	0.11	1	$\frac{3}{2}^-$ [o]	0.17	0.20	0.07	0.17
0.740	0.05	2	$\frac{3}{2}^+$ [j]	(0.26)		0.41	0.36
				$E_{He^3}=10$ MeV			
1.659	0.38	0	$\frac{1}{2}^+$	0.08	0.76	0.38	0.21
	1.37	1[m] 1	$\frac{3}{2}^-, \frac{1}{2}^-$	0.71			0.50
2.178	0.22	3	$\frac{7}{2}^-, \frac{5}{2}^-$	0.98		0.53	0.79
2.204[n]							0.63
2.265	1.26	1	$\frac{3}{2}^-, \frac{1}{2}^-$	0.59		0.35	0.55
2.308	2.50	1	$\frac{3}{2}^-$[k]	1.16	1.88	0.67	1.31
2.820[m,n]		3[m]	$(\frac{5}{2}^-)$ [n]			0.43	0.79
3.137[n]		4[n]	$\frac{9}{2}^+$ [n]				0.25
3.248[n]		0[n]	$\frac{1}{2}^+$ [n]				0.01
3.401[n]		1[n]				0.05	0.02
3.748[n]		1[m,n]				0.05	0.08
3.756	0.22	1	$\frac{3}{2}^-, \frac{1}{2}^-$	0.09			
3.763[n]		3[m,n]				0.12	0.18
3.920	0.66	1	$\frac{3}{2}^-, \frac{1}{2}^-$	0.27	0.28	0.16	0.29
4.008	0.10	1	$\frac{3}{2}^-, \frac{1}{2}^-$	0.04		0.03	0.04
4.135[n]		3[n]	$(\frac{5}{2}^-)$				0.10
4.220							0.08
4.249	0.43	1	$\frac{3}{2}^-, \frac{1}{2}^-$	0.17	0.26	0.07	0.05
4.384	0.20	1	$\frac{3}{2}^-, \frac{1}{2}^-$	0.07		0.02	0.04
4.513	0.53	1	$\frac{3}{2}^-, \frac{1}{2}^-$	0.21		0.13	0.22
4.651	0.37	1, 3[m,n]	$\frac{3}{2}^-, \frac{1}{2}^-$	0.15		0.75	2.11
4.868	0.56	1	$\frac{3}{2}^-, \frac{1}{2}^-$	0.22		0.13	0.27

TABLE III (*Continued*)

Excitation[a] energy (MeV)	Peak[b] cross section (mb/sr)	l	J^π	Spectroscopic strength $(2J+1)C^2S$ This work[c]		Other work
$Ti^{50}(He^3, d)V^{51}$				$E_{He^3}=10$ MeV	10 MeV[d]	10 MeV[p]
0	0.70	3	$\frac{7}{2}^-$	6.0	6.0	5.6
0.930[p]	0.10[p]	1[p]	$\frac{3}{2}^-$[o]			0.05
2.414	3.08	1	$\frac{3}{2}^-$[k]	1.81	2.28	1.7
2.544	0.28	0	$\frac{1}{2}^+$	0.06		0.06
2.667[p]	0.03[p]	2[p]	$\frac{3}{2}^+$[j]			0.06
3.082	0.20	3	$\frac{5}{2}^-, \frac{7}{2}^-$	1.43		0.75
3.210	1.10	1	$\frac{3}{2}^-, \frac{1}{2}^-$	0.58	0.72	0.52
3.660[p]	0.13[p]	1[d,p]			0.14	0.04
4.226[p]	0.12[p]	1[p]				0.03
4.258	1.16	1	$\frac{3}{2}^-, \frac{1}{2}^-$	0.50	0.50	0.25
4.445[p]	0.05[p]	3[p]				0.14
4.521[p]	0.09[p]	3[p]				0.22
4.633[p]	0.10[p]	3[p]				0.30
4.762	0.20	3	$\frac{5}{2}^-, \frac{7}{2}^-$	1.18		0.89
4.855	0.79	1	$\frac{3}{2}^-, \frac{1}{2}^-$	0.33		0.18
4.964[p]		1				0.24
4.990	0.90	0[p]	$\frac{1}{2}^-, \frac{3}{2}^-$	0.37		
5.104[p]						0.01
$Cr^{50}(He^3, d)Mn^{51}$				$E_{He^3}=9.5$ MeV	12 MeV[q]	
0	0.02	3	$\frac{5}{2}^-$[r]	0.21		
0.240	0.28	3	$\frac{7}{2}^-$[i]	2.62	2.33	
1.160[q]	0.01[q]					
1.495	0.02	3	$\frac{7}{2}^-, \frac{5}{2}^-$	0.16		
1.830	0.80	1	$\frac{3}{2}^-$[k]	0.75	0.63	
1.963	0.36	1	$\frac{3}{2}^-, \frac{1}{2}^-$	0.33	0.21	
2.147	0.60	1	$\frac{3}{2}^-, \frac{1}{2}^-$	0.54	0.35	
2.288	0.16	0	$\frac{1}{2}^+$	0.05	0.06	
2.426	0.02	3[q]			0.09	
2.844	0.41	1	$\frac{3}{2}^-, \frac{1}{2}^-$	0.39	0.20	
2.920	0.09	1	$\frac{3}{2}^-, \frac{1}{2}^-$	0.08	0.06	
2.985	0.05	1, 2[q]	$\frac{3}{2}^-, \frac{1}{2}^-$	0.04	0.15	
3.058	0.16	1	$\frac{3}{2}^-, \frac{1}{2}^-$	0.13	0.04	
3.150	0.03					
3.302	0.33	3	$\frac{5}{2}^-$[s]	2.69	0.84	
3.435	0.07	1	$\frac{3}{2}^-, \frac{1}{2}^-$	0.06	0.03	
3.562	0.30	1	$\frac{3}{2}^-, \frac{1}{2}^-$	0.25	0.06	
$Cr^{52}(He^3, d)Mn^{53}$				$E_{He^3}=9.5$ MeV	11 MeV[p]	22 MeV[t]
0	0.30	3	$\frac{7}{2}^-$[i]	3.34	4.10	3.76
0.383	0.01		$\frac{5}{2}^-$			
1.296	0.13	1	$\frac{3}{2}^-$[u]	0.21	0.24	0.28
2.370	0.09[p]	1[p]			0.04	
2.410	1.46	1	$\frac{3}{2}^-$[k]	1.74	1.70	1.80
2.677	0.32	1	$\frac{1}{2}^-$[v]	0.42	0.31	0.36
2.720	0.02	0	$\frac{1}{2}^+$	0.02	0.05	
2.886	0.08	1	$\frac{3}{2}^-$[w]	0.10	0.69	0.08
3.010	0.01	(2, 3)[p]			(0.05, 0.08)	
3.065	0.01	3	$\frac{5}{2}^-, \frac{7}{2}^-$	0.09	0.13	0.24

TABLE III (*Continued*)

Excitation[a] energy (MeV)	Peak[b] cross section (mb/sr)	l	J^π	Spectroscopic strength $(2J+1)C^2S$ This work[c]	Other work	
3.065	0.01	3	$\frac{5}{2}^-, \frac{7}{2}^-$	0.09	0.13	0.24
3.113	0.08	1	$\frac{3}{2}^-$[w]	0.09	0.06	0.08
3.496	0.28	1	$\frac{3}{2}^-, \frac{1}{2}^-$	0.30	0.30	0.28
3.679	0.28	3	$\frac{5}{2}^-$[s]	2.63	1.30	2.34
3.897	0.18	1	$\frac{3}{2}^-, \frac{1}{2}^-$	0.16	0.08	0.08
3.977	0.05	0	$\frac{1}{2}^+$	0.05		
4.075	0.15	3[p,t]	$\frac{3}{2}^-, \frac{1}{2}^-$	0.13	0.43	1.02
		1			0.06	0.06
4.214	0.01	1	$\frac{3}{2}^-, \frac{1}{2}^-$	0.01		
4.290	0.05	3		0.36	0.92	0.42
4.304[p]		3[p]			0.16	
4.346	0.11	1, (0)[p]	$\frac{3}{2}^-, \frac{1}{2}^-$	0.09	(0.04)	
4.446	0.39	1	$\frac{1}{2}^-, \frac{3}{2}^-$	0.36	0.22	0.28
4.583	0.16	3[t]	$\frac{1}{2}^-, \frac{3}{2}^-$	0.15	0.10	0.24
		1				0.10
4.737	0.52	1	$\frac{1}{2}^-, \frac{3}{2}^-$	0.48	0.28	0.40
4.800	0.06	(1), (0)[p]		(0.06)	(0.03)	
4.936	0.11[p]	3[p,t]			0.29	0.90
4.967	0.36	1	$\frac{1}{2}^-, \frac{3}{2}^-$	0.34	0.18	0.14
5.105	0.25	1	$\frac{1}{2}^-, \frac{3}{2}^-$	0.23	0.12	0.16
5.310	0.11	0	$\frac{1}{2}^+$	0.06	0.03	
5.485	0.11[p]	1[p]			0.05	
$Cr^{54}(He^3, d)Mn^{55}$				$E_{He^3}=8$ MeV		
0	0.003	3	$\frac{5}{2}^-$[o]	0.21		
0.126	0.09	3	$\frac{7}{2}^-$[o]	4.00		
1.533	0.10	1	$\frac{3}{2}^-$[x]	0.59		
				$E_{He^3}=9.5$ MeV		
2.266	1.05	1	$\frac{3}{2}^-$[k]	1.73		
2.575	0.29	1	$\frac{3}{2}^-, \frac{1}{2}^-$	0.46		
3.044	0.30	1	$\frac{3}{2}^-, \frac{1}{2}^-$	0.46		
3.195	0.08	3	$\frac{5}{2}^-, \frac{7}{2}^-$	1.14		
3.449	0.25	1	$\frac{3}{2}^-, \frac{1}{2}^-$	0.32		
3.546	0.37	1	$\frac{3}{2}^-, \frac{1}{2}^-$	0.46		
3.631	0.32	3	$\frac{5}{2}^-$[v]	4.07		
4.022	0.30	1	$\frac{1}{2}^-, \frac{3}{2}^-$	0.36		
4.249	0.07	1	$\frac{1}{2}^-, \frac{3}{2}^-$	0.08		
(4.404)	(0.02)	(3)		(0.17)		
4.512	0.12	1	$\frac{1}{2}^-, \frac{3}{2}^-$	0.13		
4.682	0.31	1	$\frac{1}{2}^-, \frac{3}{2}^-$	0.31		
4.796	0.15	1	$\frac{1}{2}^-, \frac{3}{2}^-$	0.14		

[a] Only levels excited in (He^3, d) reactions are listed. The excitation energies are from present work. Their accuracy is within 10 keV for the levels below 3.5 MeV, and 15 keV for the levels above 3.5 MeV.

[b] The uncertainties in cross sections are about 20%.

[c] The errors are estimated to be 25%. The $l=0$ and $l=2$ states were assumed to be $2s_{1/2}$ and $1d_{3/2}$ hole states.

[d] Reference 17.

[e] Reference 5.

[f] Reference 8.

[g] Spin-$\frac{1}{2}$ is excluded by observations of the β decay to the Ti^{47} ground state with $J^\pi=\frac{5}{2}^-$.

[h] According to systematics and theoretical predictions there should be a $\frac{5}{2}^-$ state in the vicinity of the ground state. This level is the only candidate for it. Furthermore, it is only weakly excited in (He^3, d) reactions, and is populated together with the $\frac{3}{2}^-$ ground state by the γ-ray transition from the $\frac{3}{2}^+$, 0.267-MeV level.

[i] The level contains almost full $j=\frac{7}{2}$ single-particle strength.

[j] $d_{3/2}$ hole state in agreement with systematics.

[k] Spin $\frac{1}{2}$ is excluded by the large spectroscopic strength. If $J^\pi=\frac{1}{2}^-$, this level would exhaust almost all of the $p_{1/2}$ single-particle strength and the $p_{1/2}$ centroid energy would be lower than the $p_{3/2}$.

[l] Doublet with a width of 40 keV.

[m] Reference 9.

[n] Reference 10.

[o] Reference 11.

[p] Reference 6.

[q] Reference 7.

[r] Spin $\frac{7}{2}^-$ is excluded by observation of β decay to Cr^{51} $\frac{7}{2}^-$ and $\frac{3}{2}^-$ levels.

[s] The $f_{7/2}$ strength is already exhausted by lower levels.

[t] Reference 31.

[u] P. H. Vuister, Nucl. Phys. **A91**, 521 (1967).

[v] D. D. Armstrong, A. G. Blair, H. C. Thomas, Phys. Rev. **155**, 1254 (1967).

[w] Spin $\frac{1}{2}^-$ is excluded by observation of γ-ray transitions to the $\frac{7}{2}^-$ ground state and $\frac{5}{2}^-$ 0.383-MeV level.

[x] Reference 25.

TABLE IV. Centroid energies and total spectroscopic strengths for $T_<$ states.

State	Nucleus	Energy levels[a] (MeV)	$\Sigma_i (2J+1)C^2S_i$ Expt.	Theor.	$\bar{E}_J$ (MeV)	W_J (MeV)	Sc^{49} [b] $\bar{E}_J$ (MeV)	W_J (MeV)
$1f_{7/2}$	V^{47}	0.15	4.8	4.7	0.15	0	0	0
	V^{49}	0, 218	5.9	5.6	0.36	0.8		
	V^{51}	0	6.0	6.0	0	0		
	Mn^{51}	0.24, 1.50	2.8	3.3	0.31	0.3		
	Mn^{53}	0	3.3	4.0	0	0		
	Mn^{55}	0.13	4.0	4.0	0.13	0		
$2p_{3/2}$	V^{47}	0–3.37	2.7	2.7	2.1	1.0	3.5	0.7
	V^{49}	0–4.38	3.3	3.2	2.4	1.0		
	V^{51}	0–4.85	3.3	3.4	3.1	1.0		
	Mn^{51}	0–3.59	2.6	2.7	2.4	0.6		
	Mn^{53}	0–4.35	3.3	3.2	2.8	0.7		
	Mn^{55}	0–3.55	4.0	3.7	2.5	0.6		
$1f_{5/2}$	V^{47}	2.54–3.37	3.6(5.2[c])	4.0	>2.7(2.9[c])	...	4.7	0.7
	V^{49}	...	...	4.8		...		
	V^{51}	3.08, 4.76	2.6	5.1	>3.8	...		
	Mn^{51}	0, 3.32	2.9	4.0	>3.1	...		
	Mn^{53}	3.68	2.6	4.8	>3.7	...		
	Mn^{55}	3.20, 3.63	5.4	5.1	3.4	0.7		
$2p_{1/2}$							6.0	0.6

[a] Energy levels included in summation.
[b] Reference 3.
[c] Including 3.24 level with $l=2$ or 3 assignment.

8–13.[25–30] In this work new levels were found in Mn^{55} between 4- and 5-MeV excitation.

Table III also includes (He^3, d) results obtained by other laboratories. A complete list of spectroscopic strengths is represented, while the l assignments are quoted only if different from ours. A few weakly excited levels unobserved by us were seen by others, the reason being higher incident energy and, consequently, larger cross sections. The l assignments of different laboratories in general agree with one another. However, a few differences exist. For instance, the 3.241-MeV level in V^{47} is clearly seen in our work and is not a contaminant of Ti^{48}(He^3, d) as supposed elsewhere.[8] Our angular distribution for the 1.667-MeV level of V^{47} and the 1.659-MeV level of V^{49} can be fitted only by a mixture of $l=0$ and $l=1$ angular distributions (Fig. 3), and the two levels are accordingly interpreted as doublets of $\frac{1}{2}^+$ and $\frac{3}{2}^-$ (or $\frac{1}{2}^-$) states.

We now compare the spectroscopic strengths obtained by different laboratories. Recall that we used normalization constant $N=2.6$, while MIT, Pennsylvania, and Heidelberg groups used $N=4.42$, Armstrong and Blair[31] used $N=3.8$, and St.-Pierre *et al.*[17] used $N=3.1$. Our spectroscopic strengths are in over-all agreement with at least one set of other data. For V^{47} they agree with Pennsylvania,[8] but not with MIT[5]; for V^{49} they agree with Heidelberg[10] but not with Pennsylvania,[9] and for V^{51} and Mn^{53} they agree with MIT.[6] The MIT spectroscopic strengths for V^{47} are smaller than ours and so are Pennsylvania's for V^{49}. In both cases, the difference can be attributed to the choice of the normalization constants which differ by a factor of 1.7. It is strange, however, that agreement exists elsewhere in spite of the different normalization constants. This agreement is especially puzzling for V^{51}, where MIT experiments and ours were performed at the same incident energy, and the experimental cross sections and the optical-model parameters are nearly the same in both studies.

[25] A. W. Barrows, R. C. Lamb, D. Velkley and M. T. McEllistrem, Nucl. Phys. **A107**, 153 (1968).
[26] M. A. Abuzeid, M. I. El-Zaiki, N. A. Mansour, A. I. Popov, H. R. Saad, and V. E. Storizhko, Z. Physik **199**, 506 (1967).
[27] S. E. Arnell and S. Sterner, Arkiv Fysik **26**, 309 (1964).
[28] I. M. Szöghy, B. Čujec, and R. Dayras (to be published).
[29] P. H. Vuister, Nucl. Phys. **83**, 593 (1966).
[30] L. Jonsson, O. Skeppstedt and S. E. Arnell, Arkiv Fysik **32**, 549 (1966).
[31] D. D. Armstrong and A. G. Blair, Phys. Rev. **140**, B1226 (1965).

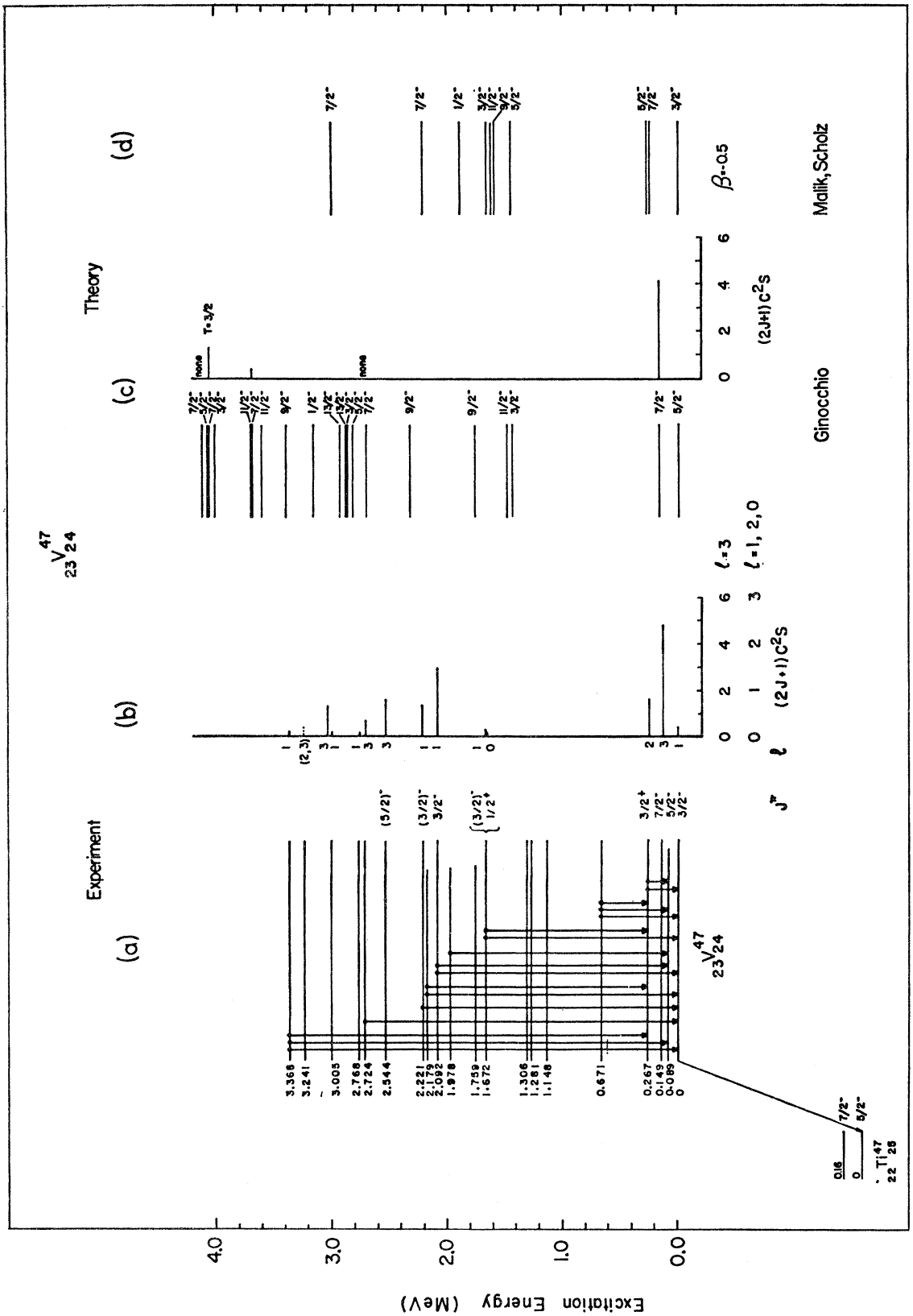

FIG. 8. Experimental and theoretical results for V^{47}. (a) Experimental energy spectrum. Energy levels $E_x \leq 2.221$ MeV (Ref. 12), $E_x \geq 2.221$ MeV (present work), γ-ray transitions (Ref. 13). For spin values see Table III. (b) Spectroscopic strengths from $Ti^{46}(He^3, d)V^{47}$. (c) Theoretical spectrum within $f_{7/2}{}^7$ configuration and $f_{7/2}-$spectroscopic strengths. (d) Theoretical spectrum in Coriolis strong-coupling model with deformation parameter $\beta = -0.5$.

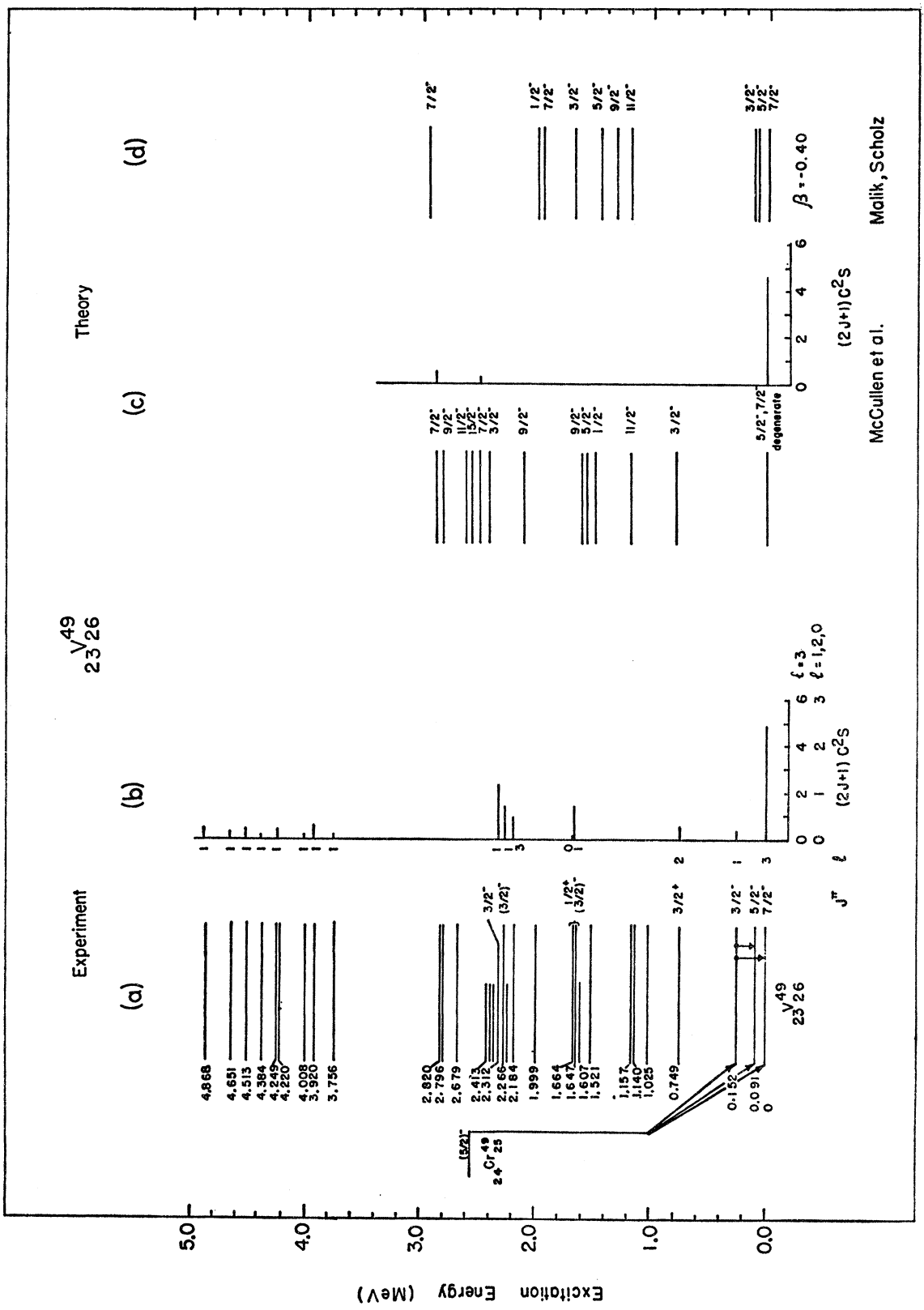

FIG. 9. Experimental and theoretical results for V^{49}. (a) Experimental energy spectrum. Energy levels $E_x \leq 2.820$ MeV (Ref. 12), $E_x \geq 3.756$ MeV (present work). For spin values, see Table III. and Ref. 11. (b) Spectroscopic strengths from $Ti^{48}(He^3, d)V^{49}$. (c) Theoretical spectrum within $f_{7/2}{}^9$ configuration and $f_{7/2}$ spectroscopic strengths. (d) Theoretical spectrum in Coriolis strong-coupling model with deformation parameter $\beta = -0.40$.

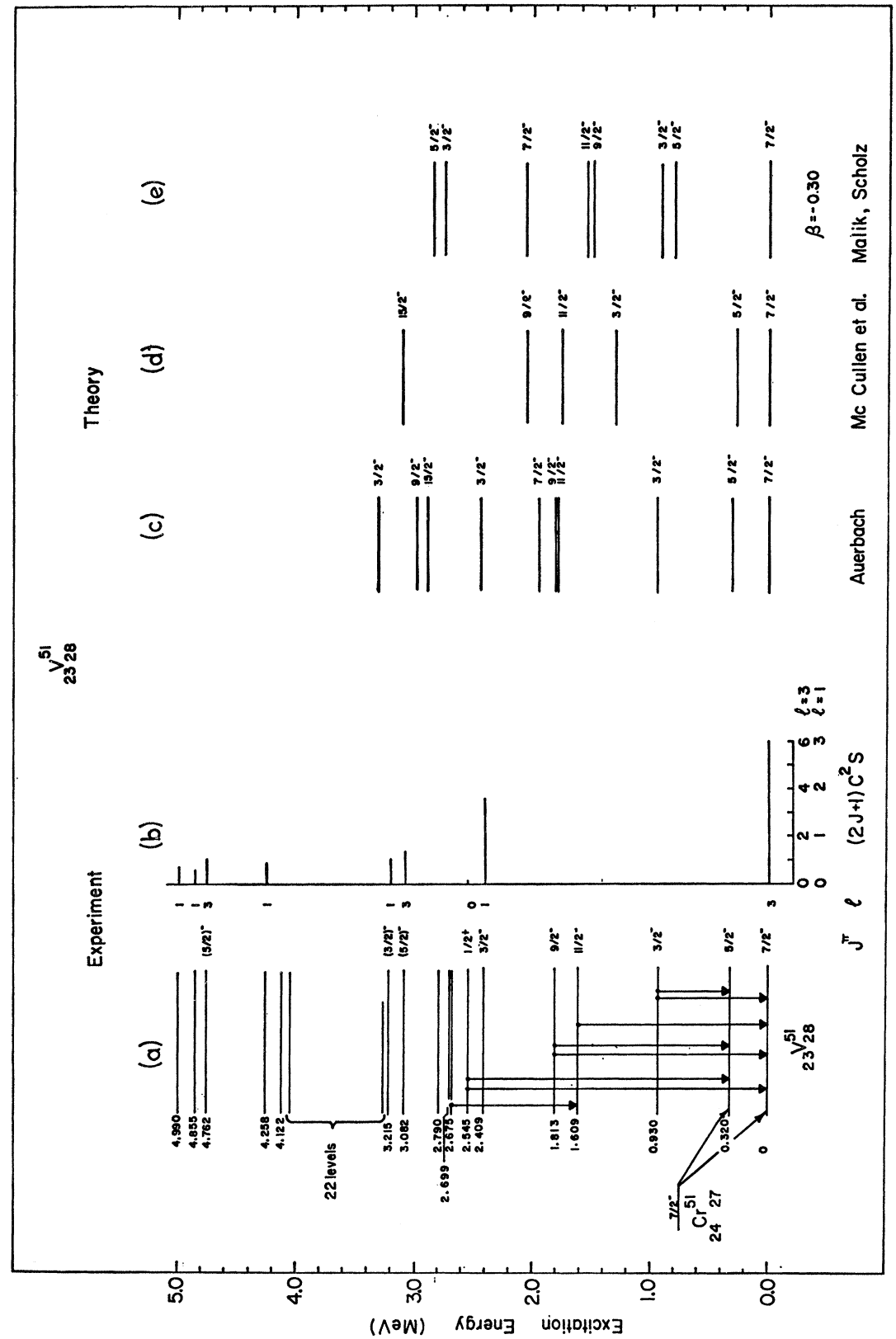

FIG. 10. Experimental and theoretical results for V^{51}. (a) Experimental energy spectrum. Energy levels $E_x \leq 4.122$ MeV and γ-ray transitions (Ref. 11). Energy levels $E_x > 4.122$ MeV (present work). For spin values, see Table III and Ref. 25. (b) Spectroscopic strengths from $Ti^{50}(He^3, d)$. (c) Theoretical spectrum within $f_{7/2}{}^3$ and $f_{7/2}{}^2p_{3/2}$ proton configurations. (d) Theoretical spectrum within pure $f_{7/2}{}^3$ proton configuration. (e) Theoretical spectrum in Coriolis strong-couping model with deformation parameter $\beta = -0.30$.

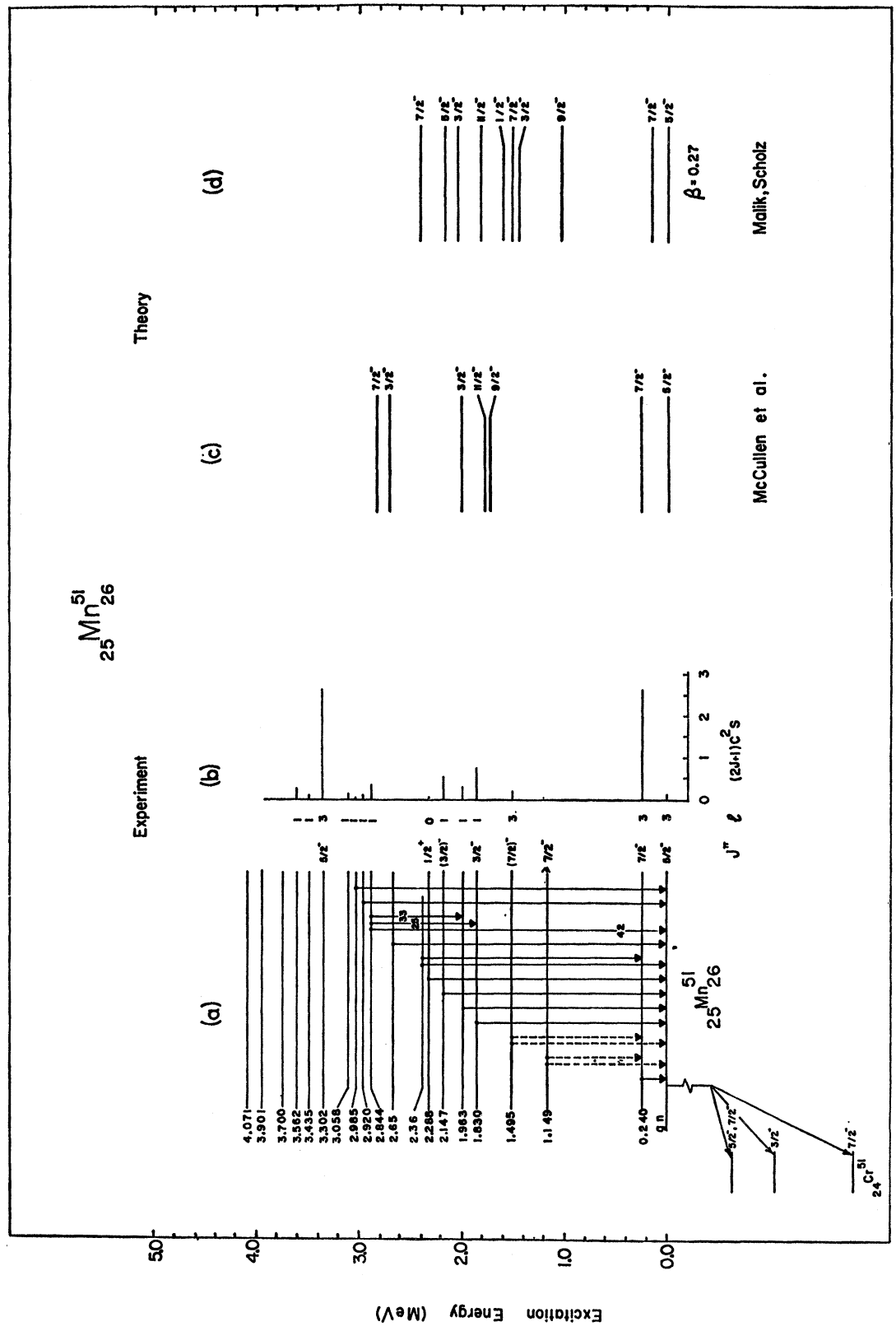

FIG. 11. Experimental and theoretical results for Mn^{51}. (a) Experimental energy spectrum. Energy levels (Refs. 14, 15 and present work). Gamma-ray transitions (Refs. 26, 27). For spin values, see Table III. (b) Spectroscopic strengths from $Cr^{50}(He^3, d)Mn^{51}$. (c) Theoretical spectrum within $f_{7/2}{}^{11}$ configuration. (d) Theoretical spectrum in Coriolis strong-coupling model with deformation parameter $\beta=0.27$.

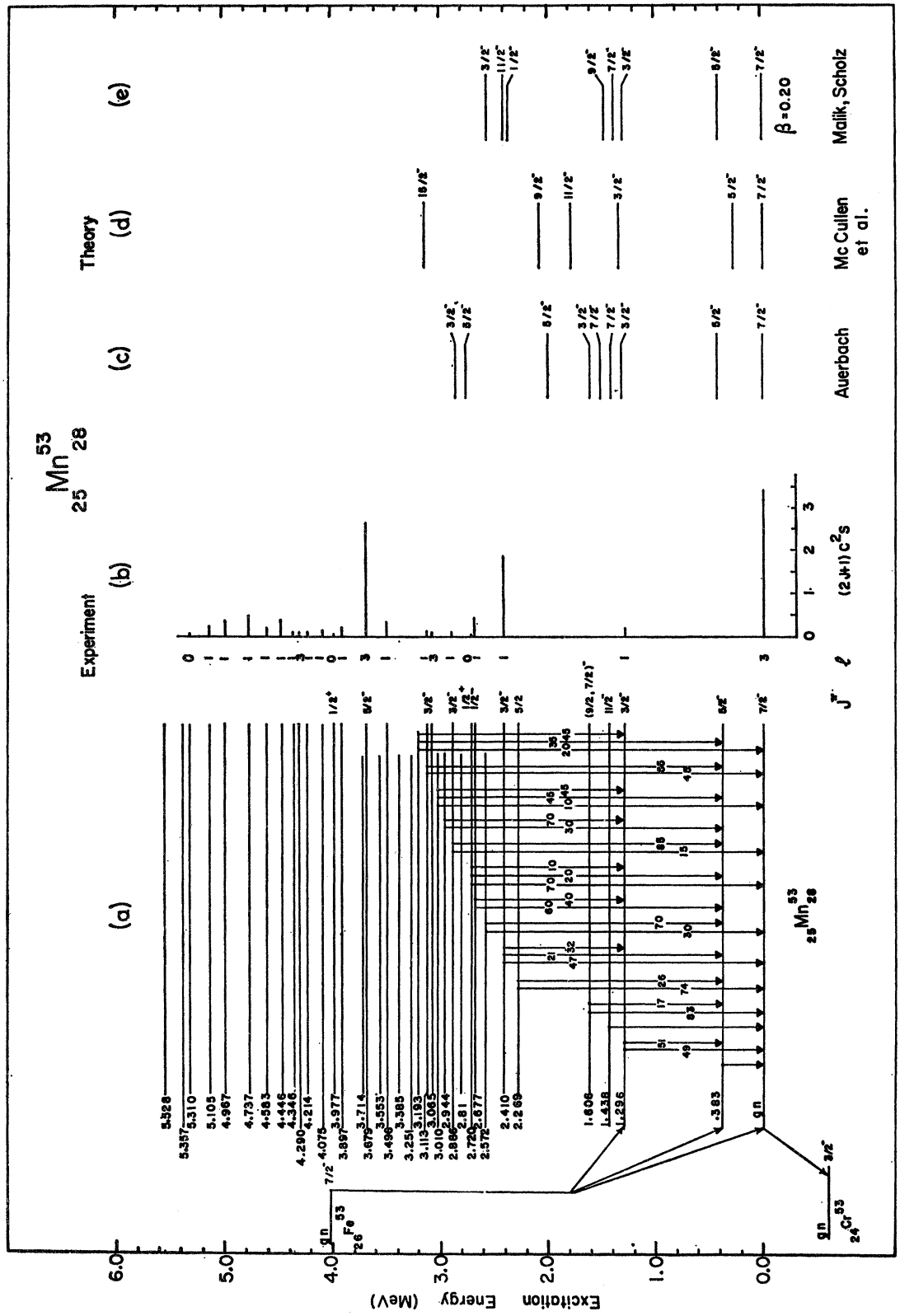

FIG. 12. Experimental and theoretical results for Mn^{53}. (a) Experimental energy spectrum. Energy levels (Ref. 14 and present work). Gamma ray transitions $E_x < 2.410$ MeV (Ref. 28) $E_x > 2.410$ (Ref. 29). For spin values, see Table III and Ref. 28. (b) Spectroscopic strengths from $Cr^{52}(He^3, d)Mn^{53}$. (c) Theoretical spectrum within $f_{7/2}{}^{-3}$ and $f_{7/2}{}^{-4}p_{3/2}$ proton configurations. (d) Theoretical spectrum within pure $f_{7/2}{}^{-3}$ proton configuration. (e) Theoretical spectrum in the Coriolis strong-coupling model with the deformation parameter $\beta = 0.20$.

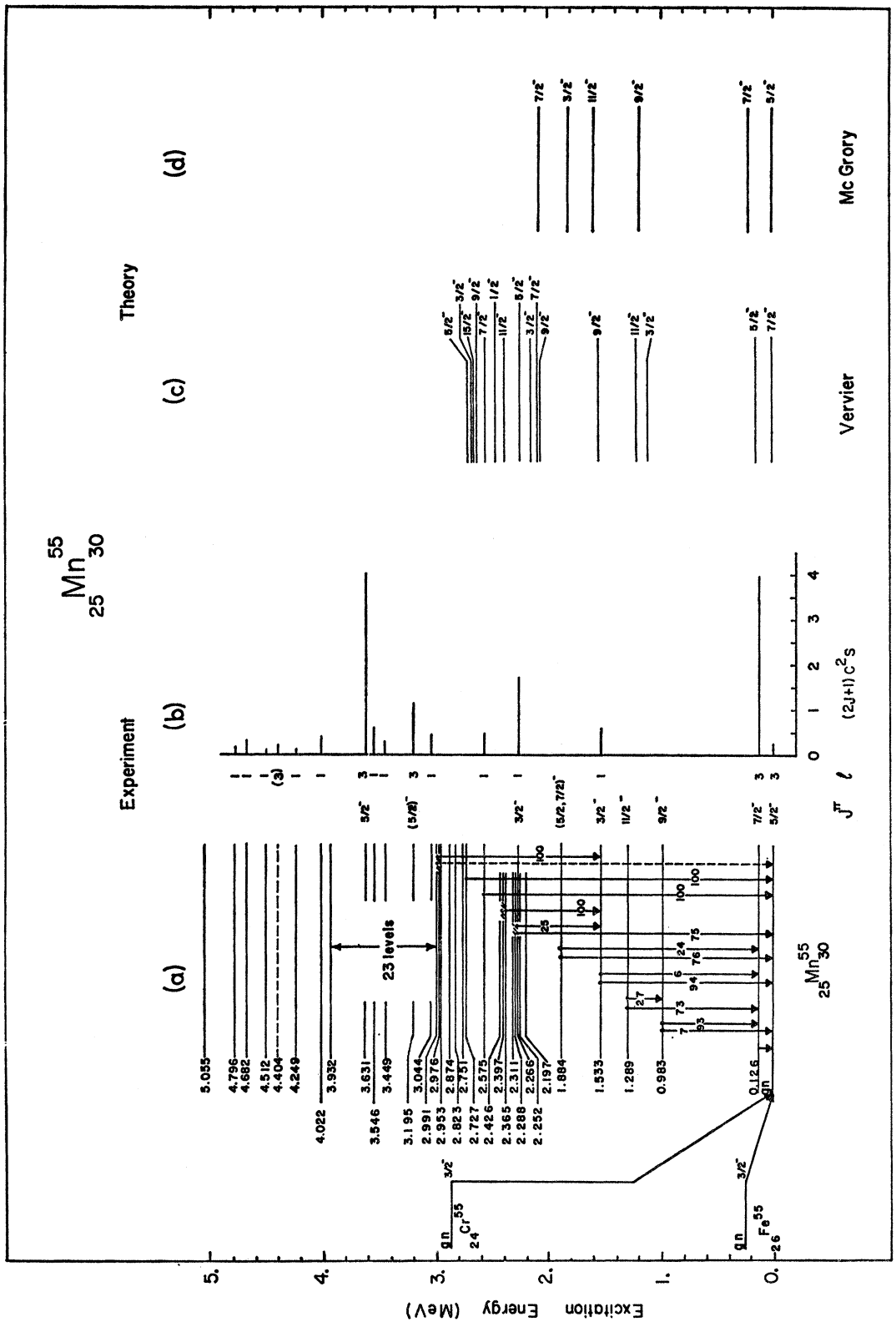

FIG. 13. Experimental and theoretical results for Mn^{55}. (a) Experimental energy spectrum. Energy levels (Ref. 11 and present work). Gamma-ray transitions $E_x < 1.884$ MeV (Ref. 28), $E_x > 1.884$ MeV (Ref. 30). For spin values, see Table III and Ref. 25. (b) Spectroscopic strengths from $Cr^{54}(He^3, d)Mn^{55}$. (c) Theoretical spectrum within $(f_{7/2})^{-3}$ proton and $(2p_{3/2})^2$ neutron configurations. (d) Theoretical spectrum within $(f_{7/2})^{-3}$ proton and $(2p_{3/2})^2$, $(2p_{1/2})^2$, $(1f_{5/2})^2$ neutron configurations.

TABLE V. $d_{3/2}$ and $s_{1/2}$ proton hole states.

Nucleus	$E_x(d_{3/2}^{-1})$ Expt.[a]	$E_x(d_{3/2}^{-1})$ Theor.[b]	$E_x(s_{1/2}^{-1})$ Expt.[a]	$E_x(s_{1/2}^{-1})$ Theor. (b)	$E_x(s_{1/2}^{-1})$ Theor. (c)	$E_x(d_{3/2}^{-1})-E_x(s_{1/2}^{-1})$ Expt.[a]	$E_x(d_{3/2}^{-1})-E_x(s_{1/2}^{-1})$ Theor. (b)	$E_x(d_{3/2}^{-1})-E_x(s_{1/2}^{-1})$ Theor. (c)
V^{47}	0.263	0.40	1.664	1.16	1.72	1.401	0.76	1.32
V^{49}	0.748	1.04	1.653, 1.999	1.24	1.94	0.905	0.20	0.90
V^{51}	2.671	2.02	2.543	1.66	2.50	−0.128	−0.36	0.48
Mn^{51}	2.985	1.58	2.30	1.42	2.26	−0.371	−0.16	0.68
Mn^{53}		1.99	2.72	1.27	2.25		−0.72	0.26

[a] The mean value from all high-resolution data.
[b] The parameters are from Reference 34: $\langle E^{(2)}\rangle_{av}(d_{3/2}-f_{7/2}) = -0.25$ MeV, $\langle \Delta E^{(2)}\rangle_{av}(d_{3/2}-f_{7/2}) = 2.8$ MeV; $\langle E^{(2)}\rangle_{av}(s_{1/2}-f_{7/2}) = -0.02$ MeV, $\langle \Delta E^{(2)}\rangle_{av}(s_{1/2}-f_{7/2}) = 2.6$ MeV.
[c] The same as (b) except for $\langle E^{(2)}\rangle_{av}(s_{1/2}-f_{7/2}) = -0.09$ MeV.

Also some relative differences in spectroscopic strengths are present, which cannot be attributed to the difference in normalization constant or optical-model parameters. As an example, consider the three relatively strongly excited $l=1$ levels of Mn^{51} at 1.830, 1.963, and 2.147 MeV. The relative spectroscopic strengths for the second and third levels with respect to the first (100%) are 43 and 70% in our work, and only 33 and 56% in the MIT work. For these three levels, we have data at 8.5, 9.5- and 10.5-MeV bombarding energies, with the relative spectroscopic strengths in agreement within 3%.

The measured l value in general allows two possibilities, $J=l\pm\frac{1}{2}$, for the spin of the final state. In several cases, however, a unique assignment can be made on the basis of the shell-model systematics, or in combination with the observed β- and γ-ray transitions. For instance, the most strongly excited $l=1$ level, observed with each of these nuclei between 2- and 2.5-MeV excitation, has $J^\pi=\frac{3}{2}^-$, since the $p_{3/2}$ single-particle state lies below the $p_{1/2}$ state. If $J^\pi=\frac{1}{2}^-$, this level would exhaust almost all of the $p_{1/2}$ single-particle strength and the $p_{1/2}$ centroid energy would be lower than the $p_{3/2}$. An $l=1$ level, for which a γ-ray transition to the $\frac{7}{2}^-$ level is observed, has also $J^\pi=\frac{3}{2}^-$, since in the opposite case of $J^\pi=\frac{1}{2}^-$ this transition would be $M3$ and would not compete with the $M1$ and $E2$ transitions to the $\frac{5}{2}^-$ and $\frac{3}{2}^-$ levels. These and similar arguments were applied in assignment of unique spin values to several levels in Table III.

The total spectroscopic strength for transferring a proton to a target with $J_0=0$ into an orbit j, and forming the levels with $J=j$ and $T=T_0-\frac{1}{2}=T_<$, is theoretically given by[32]

$$\sum_i (2J+1)C^2S_i = \langle p\rangle_j - [\langle n\rangle_j/(2T_0+1)], \quad (1)$$

where $\langle p\rangle_j$ and $\langle n\rangle_j$ are the number of proton and neutron holes in this same j orbit, and $T_0=\frac{1}{2}(N-Z)$ is the isospin of the target nucleus. We used this theoretical value as a guide in calculating the centroid energies

$$\bar{E}(J) = \sum_i (2J+1)C^2S_iE_i / \sum_i (2J+1)C^2S_i \quad (2)$$

and spreading widths

$$W(J) = \left[\frac{\sum_i (2J+1)C^2S_i[E_i(J)-\bar{E}(J)]^2}{\sum_i (2J+1)C^2S_i}\right]^{1/2}. \quad (3)$$

We included sufficient of the first $l=1$ states into summation to get their total spectroscopic strength closest to the theoretical value. The results thus obtained are reasonable (Table IV). The centroid energies are consistent with the average $p_{3/2}-f_{7/2}$ two-body interaction of Schwartz.[33] Within the same isotope, the centroid energies increase when adding neutrons. The exception is Mn^{55}, where the last two neutrons come in the $p_{3/2}$ orbit. The decrease of the centroid energy is explained by the especially strong interaction between a proton and a neutron when in the same orbit.

The $\frac{3}{2}^+$ and $\frac{1}{2}^+$ low-lying states of vanadium and manganese isotopes are believed to be $1d_{3/2}$ and $2s_{1/2}$ proton hole states. The evidence for this comes (1) from the relatively weak excitation in the (He^3, d) reactions, (2) from the strong excitation in the proton pickup reactions such as[10] $Cr^{50}(t,\alpha)$ V^{49}, and (3) from the γ-ray transitions, such as in V^{51}. The $\frac{1}{2}^+$ state of V^{51} at 2.545 MeV is observed[11] to decay to the $\frac{7}{2}^-$ ground state and to the $\frac{5}{2}^-$ state at 0.320 MeV. No γ ray is observed to the $\frac{3}{2}^-$ state at 0.930 MeV, though this would be an $E1$ transition, in contrast to the observed $E3$ transitions. As the single-particle transition $f_{7/2}\rightarrow s_{1/2}$ has to be of $E3$ type, this indicates that the initial state and the three final states under con-

[32] J. B. French and M. H. Macfarlane, Nucl. Phys. **26**, 168 (1961).

[33] J. J. Schwartz, Phys. Letters **24B**, 224 (1967).

sideration are very pure shell-model states, $s_{1/2}^{-1}f_{7/2}^{4}$ and $f_{7/2}^{3}$, respectively.

The experimentally observed low-lying $\frac{3}{2}^+$ and $\frac{1}{2}^+$ states are represented in Table V. Some additional $l=2$ and $l=0$ states were found,[10] lying more than 2.5 MeV above these $d_{3/2}^{-1}$ and $s_{1/2}^{-1}$ states, being probably of a different character. Thus we reasonably assume that the listed levels more or less coincide with the so-called centroid energies of the $d_{3/2}^{-1}$ and $s_{1/2}^{-1}$ states. Following Bansal and French,[34] these centroid energies are easily calculable and depend only on two parameters: the average two-body interaction $\langle E^{(2)}\rangle_{\mathrm{av}}$ and the average difference $\langle \Delta E^{(2)}\rangle_{\mathrm{av}}$ for these interactions when the two nucleons are in the isospin state $T=0$ and $T=1$. With the parameters extracted[34] from scandium isotopes, the centroid energies of column (b), Table V, are calculated. Better agreement is achieved in column (c) where the parameter $\langle F^{(2)}\rangle_{\mathrm{av}}(s_{1/2}-f_{7/2})$ was changed from -0.02 to -0.09 MeV.

COMPARISON OF EXPERIMENTAL RESULTS WITH THEORETICAL MODELS

Several calculations of energy spectra, based on the shell model and on the strong-coupling model, are available in this region. McCullen *et al.*[21] and Ginnocchio[22] performed shell-model calculations for protons and neutrons in the $f_{7/2}$ configurations. Vervier[35] and McGrory[36] did similar calculations for $N=30$ nuclei ($_{25}Mn_{30}^{55}$). Auerbach[37] calculated the energy spectra for nuclei with neutrons in closed shell ($N=28$), considering $f_{7/2}^{n}$ and $f_{7/2}^{n-1}p_{3/2}$ proton configurations. On the other hand, Malik and Scholz[38] applied to these nuclei the Bohr-Mottelson strong-coupling model, including the Coriolis coupling between bands.

Figures 8–13 show the experimental and theoretical results for $V^{47,49,51}$ and $Mn^{51,53,55}$. The calculations, based on the $f_{7/2}^{n}$ configurations, can of course not predict the $l=1$ transitions. They do, however, provide two important pieces of information concerning the (He^3, d) reactions: (1) The $f_{7/2}$ strength is concentrated in just one level, just what was actually observed, and (2) all other levels predicted by these calculations should be unobserved or very weakly excited. Malik and Scholz[38] do not provide any information about the spectroscopic strengths and so the comparison of the strong-coupling model with the experimental data remains vague. The predictions of Auerbach[37] agree with the observed energy levels and spectroscopic strengths in the case of V^{51}, but not in the case of Mn^{53}. Actually, the spectra calculated by Malik and Scholz and by Auerbach are so similar that neither the strong-coupling nor the shell model can be excluded by the available theoretical and experimental information.

TABLE VI. $\frac{3}{2}^-$ states within $f_{7/2}^{n+1}$ and $f_{7/2}^{n}\,p_{3/2}$ configurations for nuclei with $N=28$ or $Z=20$. Theory.

Nucleus	States[a]
$_{21}Sc_{28}^{49}-{}_{20}Ca_{21}^{41}$	$p_{3/2}$
$_{23}V_{28}^{51}-{}_{20}Ca_{23}^{43}$	$f_{7/2}^{3}(0), f_{7/2}^{2}(0)\,p_{3/2}, f_{7/2}^{2}(2)\,p_{3/2}$
$_{25}Mn_{28}^{53}-{}_{20}Ca_{25}^{45}$	$f_{7/2}^{-3}, f_{7/2}^{4}(0)\,p_{3/2}, f_{7/2}^{4}(2)\,p_{3/2}, f_{7/2}^{4}(2')\,p_{3/2}$
$_{27}Co_{28}^{55}-{}_{20}Ca_{27}^{47}$	$f_{7/2}^{-2}(0)\,p_{3/2}, f_{7/2}^{-2}(2)\,p_{3/2}$

[a] The $f_{7/2}^{4}(2')$ denotes a $J=2$, seniority 4 state, while all the other $J=2$ states have seniority 2.

Therefore we use a different approach to interpret the experimental data. The most positive and reliable information we get from the (He^3, d) reactions is the location of $l=1$ states and the splitting of the $p_{3/2}$ strength. These quantities, or better, their variation with nuclei, are expected to be drastically different in the two models.

In the strong-coupling model all nucleons except for the last odd one are incorporated in the deformed core, which is characterized by two parameters: the deformation and the moment of inertia. Provided that these remain constant, the nuclei with the same number of odd nucleons are equivalent, i.e., have the same energy levels and wave functions. Under these conditions, the nuclei with Z or $Z=23$, such as $_{23}V_{24}^{47}$, $_{23}V_{26}^{49}$, $_{23}V_{28}^{51}$, and $_{20}Ca_{23}^{43}$, are equivalent, and so are the nuclei with Z or $N=25$, such as $_{25}Mn_{26}^{51}$, $_{25}Mn_{28}^{53}$, $_{25}Mn_{30}^{55}$, and $_{20}Ca_{25}^{45}$. The changes in the moment of inertia and in the deformation parameter influence the relative positions of levels, but do not change the number of levels with a certain J^π value. Up to 3 MeV excitation energy, Malik and Sholz predicted for $_{23}V^{47,49,51}$, as well as for $_{25}Mn^{51,53}$, two $\frac{3}{2}^-$ states and one $\frac{1}{2}^-$ state.

In the shell model the number of levels with a certain J^π essentially depends on the number of nucleons outside the closed shells. Table VI lists the unperturbed states with $J^\pi=\frac{3}{2}^-$ within $f_{7/2}^{n+1}$ and $f_{7/2}^{n}p_{3/2}$ configurations for nuclei with either neutrons or protons in closed shells ($N=28$ or $Z=20$). Omitting the limitation that one kind of nucleons be in closed shells, the number of unperturbed $J^\pi=\frac{3}{2}^-$ states increases rapidly (Table VII). Through the residual interaction, the unperturbed states get mixed; however, the number of states remains the same. Each physical state is in principle composed of all unperturbed states with the same J^π value, and the component (target ground)$\times p_{3/2}$ determines the spectroscopic strength for the $p_{3/2}$ transfer reactions. In particular, the $\frac{3}{2}^-$ states of $f_{7/2}^{n+1}$ configuration are observed (as $l=1$ states) via admixture with $f_{7/2}^{n}p_{3/2}$ configuration.

[34] R. K. Bansal and J. B. French, Phys. Letters **11**, 145 (1964).
[35] J. Vervier, Nucl. Phys. **78**, 497 (1966).
[36] J. B. McGrory, Phys. Rev. **160**, 915 (1967).
[37] N. Auerbach, Phys. Letters **24B**, 260 (1967).
[38] F. B. Malik and W. Scholz, Phys. Rev. **150**, 919 (1966).

TABLE VII. $\frac{3}{2}^-$ states for vanadium and manganese isotopes. Theory.

Nucleus	Configuration[a]	Number of states	E_x (MeV) for states below 3 MeV	Configuration[a]	Number of states	Lowest states[b]
$_{23}V_{28}^{51}$	$f_{7/2}{}^{3p}$	1	1.4	$f_{7/2}{}^{3p}p_{3/2}{}^{1p}$	2	$f_{7/2}{}^{3}(0)\,p_{3/2}{}^{1p}, f_{7/2}{}^{3p}(2)\,p_{3/2}{}^{1p}$
$_{23}V_{26}^{49}$	$f_{7/2}{}^{3p}f_{7/2}{}^{-2n}$	11	0.8, 2.4	$f_{7/2}{}^{3p}f_{7/2}{}^{-2n}\,p_{3/2}{}^{1p}$	23	$f_{7/2}{}^{2p}(0)\,f_{7/2}{}^{-2n}(0)\,p_{3/2}, f_{7/2}{}^{2p}(2)\,f_{7/2}{}^{-2n}(0)\,p_{3/2}$, $f_{7/2}{}^{3p}(0)\,f_{7/2}{}^{-2n}(2)\,p_{3/2}, \cdots$
$_{23}V_{24}^{47}$	$f_{7/2}{}^{3p}f_{7/2}{}^{4n}$	22	1.4	$f_{7/2}{}^{3p}f_{7/2}{}^{4n}\,p_{3/2}{}^{1p}$	47	$f_{7/2}{}^{2p}(0)\,f_{7/2}{}^{4n}(0)\,p_{3/2}, f_{7/2}{}^{2p}(2)\,f_{7/2}{}^{4n}(0)\,p_{3/2}$, $f_{7/2}{}^{3p}(0)\,f_{7/2}{}^{4n}(2)\,p_{3/2}, \cdots$
$_{25}Mn_{28}^{53}$	$f_{7/2}{}^{-3p}$	1	1.4	$f_{7/2}{}^{4p}\,p_{3/2}{}^{1p}$	3	$f_{7/2}{}^{4p}(0)\,p_{3/2}{}^{1p}, f_{3/2}{}^{4p}(2)\,p_{3/2}{}^{1p}, f_{7/2}{}^{4p}(2')\,p_{3/2}{}^{1p}$
$_{25}Mn_{26}^{51}$	$f_{7/2}{}^{-3p}f_{7/2}{}^{-2n}$	11	1.7, 2.4	$f_{7/2}{}^{4p}f_{7/2}{}^{-2n}\,p_{3/2}{}^{1p}$	47	$f_{7/2}{}^{4p}(0)\,f_{7/2}{}^{-2n}(0)\,p_{3/2}{}^{1p}, f_{7/2}{}^{4p}(2)\,f_{7/2}{}^{-2n}(0)\,p_{3/2}{}^{1p}$ $f_{7/2}{}^{4p}(0)\,f_{7/2}{}^{-2n}(2)\,p_{3/2}, \cdots$

[a] The letter p or n in exponent refers to protons or neutrons. For instance, $f_{7/2}{}^{3p}f_{7/2}{}^{-2n}$ means configuration with 3 protons and 2 neutron holes in the $f_{7/2}$ shell.

[b] The $f_{7/2}{}^{4p}(2')$ with Mn^{53} denotes a $J=2$, seniority 4 state, while all the other $J=2$ states have seniority 2.

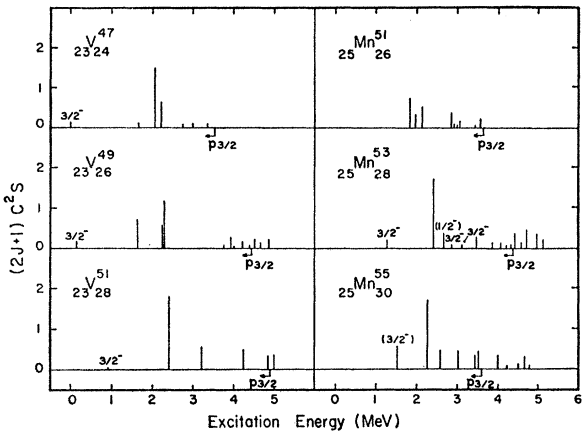

FIG. 14. Splitting of the $l=1$ spectroscopic strength in vanadium and manganese isotopes. The J^π assignments are from γ-ray measurements. The arrows mark the levels needed to exhaust the $p_{3/2}$ strengths.

Figure 14 shows the $l=1$ experimental data for vanadium and manganese isotopes. Each level is represented by the spectroscopic strength $(2J+1)C^2S$ extracted from the (He^3, d) cross section. By the departure from neutron closed shells, the splitting of the $l=1$ spectroscopic strength is clearly observed. The strongly excited level at 2.414 MeV in $_{23}V_{28}^{51}$ (neutron shells closed) is replaced in $_{23}V_{26}^{49}$ and $_{23}V_{24}^{47}$ by a group of three levels. The relation is similar between $_{25}Mn_{28}^{53}$ and $_{25}Mn_{26}^{51}$. This splitting is in contradiction with the strong-coupling model, but it is in the spirit of the shell model.

We now discuss the number of $\frac{3}{2}^-$ shell-model states expected at low excitation energies. Below 2 MeV for each of these nuclei, only one $\frac{3}{2}^-$ state is predicted within pure $f_{7/2}$ configurations, although the total number of predicted states for V^{49} and Mn^{51} is 11, and for V^{47} is 22. Similarly we expect that only few of the $\frac{3}{2}^-$ states of the $f_{7/2}{}^n p_{3/2}$ configuration will be close enough to the (target ground)$\times p_{3/2}$ state to get an appreciable amount of this last state and, consequently, of the $p_{3/2}$ strength.

First of all, this should be the states listed in the last column of Table VII. Another way to get the $\frac{3}{2}^-$ states, which are closest to the (target ground)$\times p_{3/2}$ state, is to look at the energy levels of the target nucleus. Only the 0^+, 1^+, 2^+, 3^+ target states can couple with the $p_{3/2}$ proton state to give a $\frac{3}{2}^-$ final state. In addition to the 0^+ ground state, the relevant target states below 3 MeV are one 2^+ state for Ti^{50} and Cr^{52} (1.5 MeV) and two 2^+ states for Ti^{46}, Cr^{50} (1.1 and 2.8 MeV) and Ti^{48} (1.2 and 2.0 MeV). The levels calculated[20] within $f_{7/2}$ configurations, in parentheses, agree within 0.2 MeV with experimental spectra. Accordingly, in V^{47}, V^{49}, and Mn^{51}, not many more than three states are expected to share the $p_{3/2}$ strengths, although the number of $\frac{3}{2}^-$ states is large.

We now consider the nuclei with either neutrons or

protons in closed shells ($N=28$ or $Z=20$). Here only a few states with $J^\pi=\frac{3}{2}^-$ exist within $f_{7/2}{}^{n+1}$ and $f_{7/2}{}^n p_{3/2}$ configurations, and a complete list of them is given in Table VI. Figure 15[39–42] represents the $l=1$ experimental data. The low-lying $\frac{3}{2}^-$ state of the $f_{7/2}{}^{n+1}$ configuration is present and is very weakly excited in V^{51}, Mn^{53}, Ca^{43}, and Ca^{45}, but it is absent in Sc^{49}, Co^{55}, Ca^{41}, and Ca^{47}, wholly agreeing with the shell-model predictions. The $f_{7/2}{}^n p_{3/2}$ shell-model states can be followed from Sc^{49} through V^{51} and Mn^{53} up to Co^{55}. The strongly excited state of Sc^{49} at 3.1 MeV is replaced in V^{51} by two states, and in Mn^{53} by three states with about the same total strength, which is again in agreement with the shell-model predictions. In Co^{55} several $l=1$ states are present, but already two of them exhaust the total $p_{3/2}$ strength. At least one of the low-lying strongly excited $l=1$ states is expected, by analogy with Co^{57}, Cu^{61}, and Cu^{63}, to be a $p_{1/2}$ state.

In conclusion, for the $N=28$ and $Z=20$ nuclei, the $f_{7/2}{}^{n+1}$ and $f_{7/2}{}^n p_{3/2}$ shell-model configurations describe well the splitting of the $p_{3/2}$ strength. However, they do not account for all levels. The most striking evidence for insufficiency of the shell-model configurations are

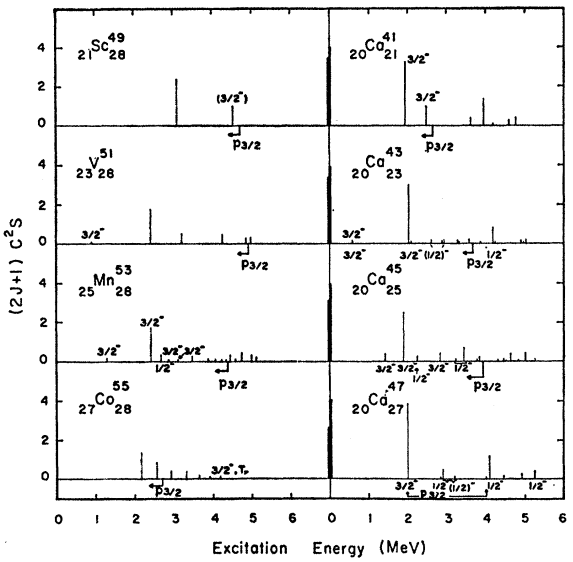

FIG. 15. Splitting of the $l=1$ spectroscopic strength for $N=28$ and $Z=20$ nuclei and comparison between proton and neutron $l=1$ strengths in equivalent pairs. The J^π assignments above the line are from γ-ray measurements, while those below the line are from "dip" observations in (d, p) and (α, t) angular distributions. All levels have $T=T_<$, except for the last level in Co^{55}. The total strength for the $T_<$ proton $p_{3/2}$ states, and the total $p_{3/2}$ strength applying to the neutron states, are marked on the central line. The data for Ca isotopes are from Refs. 39–42.

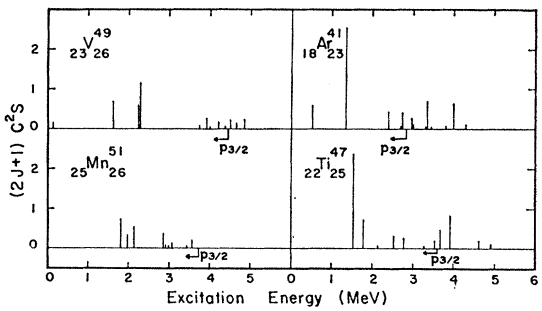

FIG. 16. Comparison between proton and neutron $l=1$ strengths in semiequivalent pairs. The arrows mark the levels needed to exhaust the $p_{3/2}$ strengths. Ar^{41} data (Ref. 43); Ti^{47} data (Ref. 44).

the two $\frac{3}{2}^-$ levels observed in both Ca^{41} and Sc^{49} nuclei. Being composed of closed shells plus one nucleon, these two nuclei can have only one $\frac{3}{2}^-$ state within the shell-model configurations. The two $\frac{3}{2}^-$ states demonstrate that the core excitation is present. Below the second $\frac{3}{2}^-$ state of Sc^{49}, a group of levels with about the same total strength appears in V^{51} and Mn^{53}, indicating that the same core excitation is present through Ca^{48}, Ti^{50}, and Cr^{52} cores.

Let us now compare the proton and the neutron $p_{3/2}$ states in equivalent pairs: $_{21}Sc_{28}^{49}$-$_{20}Ca_{21}^{41}$, $_{23}V_{28}^{51}$-$_{23}Ca_{20}^{43}$, $_{25}Mn_{28}^{53}$-$_{20}Ca_{25}^{45}$, and $_{27}Co_{28}^{55}$-$_{20}Ca_{27}^{47}$. Though the shell-model states are the same for each equivalent pair, some differences are expected due to the following two facts: (1) The single-particle states are different. For proton states (core Ca^{48}) their sequence is $f_{7/2}$, $p_{3/2}$, $f_{5/2}$, $p_{1/2}$. while for neutron states (core Ca^{40}), it is $f_{7/2}$, $p_{3/2}$, $p_{1/2}$, $f_{5/2}$. Therefore, the proton $p_{1/2}$ states are expected to be separated from $p_{3/2}$ states, at least at the beginning of the shell, while this is not the case for neutron states. (2) All of the neutron strength is concentrated in the states with the lowest isospin value, because these are the only states which can be reached in a neutron transfer. In a proton transfer, however, the states with $T=T_0-\frac{1}{2}=T_<$, as well as with $T=T_0+\frac{1}{2}=T_>$, can be reached (T_0=isospin of the target), and the spectroscopic strength is shared among the $T_<$ and $T_>$ states in a predicted way.

Experimental data (Fig. 15) reproduce these differences. In addition, they show also that the splitting of the $p_{3/2}$ strength is different. While for neutron states the $p_{3/2}$ strength is more or less concentrated in just one level, for proton states it is substantially split among several levels. This difference is expecially pronounced in the Co^{55}-Ca^{47} pair, but it is present through all equivalent pairs. Moreover, it is observed also in other nuclei, where a reasonable comparison can be made, such as in $_{23}V_{26}^{49}$-$_{18}Ar_{23}^{41}$ and $_{25}Mn_{26}^{51}$-$_{22}Ti_{25}^{47}$ pairs (Fig. 16).[43,44] This difference in splitting

[39] T. A. Belote, A. Sperduto, and W. W. Buechner, Phys. Rev. **139**, B80 (1965).
[40] W. E. Dorenbusch, T. A. Belote, and Ole Hansen, Phys. Rev. **146**, 734 (1966).
[41] J. Rapaport, W. E. Dorenbusch, and T. A. Belote, Phys. Rev. **156**, 1255 (1967).
[42] T. A. Belote, H. Y. Chen, Ole Hansen, and J. Rapaport, Phys. Rev. **142**, 624 (1966).
[43] E. Kashy, A. M. Hoogenboom, and W. W. Buechner, Phys. Rev. **124**, 1917 (1961).
[44] J. Rapaport, A. Sperduto, and W. W. Buechner, Phys. Rev. **143**, 808 (1966).

of the $p_{3/2}$ strength remains to be explained. Perhaps it can be attributed to the particle-hole configurations or so-called relaxed core excitations, which are present when adding protons, but are absent when adding neutrons.

Note added in manuscript. As the recent measurements[45] of the Sc^{42} spectrum show, the two-body matrix elements used in the calculations by McCullen *et al.* and Ginnocchio have to be modified. This modification, however, does not affect our conclusions.

[45] J. J. Schwartz, D. Cline, H. E. Gove, R. Sherr, T. S. Bnatia, and R. H. Siemssen, Phys. Rev. Letters **19**, 1482 (1967).

PHYSICAL REVIEW VOLUME 179, NUMBER 4 20 MARCH 1969

j_n Dependence of (d, p) Reactions from the Weakly Bound Projectile Model

C. A. PEARSON
Department of Physics, University of Arizona, Tucson, Arizona 85721
AND
J. M. BANG AND L. POCS*
The Niels Bohr Institute, Copenhagen, Denmark

(Received 29 July 1968)

The j_n dependence of the angular distributions for certain (d, p) reactions is calculated from the weakly bound projectile (WBP) model of Pearson and Coz. Agreement is found with the observed j_n dependence. It is suggested that the model can be used for extracting the value of j_n from accurately measured angular distributions.

I. INTRODUCTION

As emphasized by Lee and Schiffer[1,2] the measured angular distributions for (d, p) reactions on zero-spin target nuclei depend on the total angular momentum of the transferred neutron. Certain of the inverse (p, d) reactions depend in the same way on the total angular momentum j_n of the picked-up[2,3] neutron. When the measured angular distributions for two similar reactions with the same l_n but different j_n are normalized to coincide at the stripping peak, their difference shows a characteristic angular structure. Extensive efforts with conventional distorted-wave Born-approximation (DWBA) calculations have failed to reproduce this structure.[4–6]

Recently a weakly bound projectile (WBP) model for deuteron stripping reactions has been put forward by Pearson and Coz[7] (PC), who suggest that the model accounts for the main features of the observed j_n dependence.[8] PC used qualitative arguments to discuss the characteristic difference between the two stripping angular distributions referred to above. They showed that under certain circumstances this angular-dependent difference is proportional to the polarization produced when protons with the energy of the proton in the (d, p) reaction are elastically scattered from the short-range part of the proton–target-nucleus interaction.[8] (We hereafter call this simply elastic scattering.)

In this paper we present the results of detailed calculations with the WBP model, using standard nucleon-nucleus optical-model parameters.[9] We find the model gives a good account of the observed j_n dependence. The detailed calculations confirm the qualitative arguments of PC.

The calculations reported here form part of a study of the WBP model for (d, p) reactions on zero-spin target nuclei. Using the same standard set of optical-model parameters, we show elsewhere[10,11] that the model gives good agreement with the shape and magnitude of measured (d, p) angular distributions as well as with the measured proton polarization.

It seems possible that a reliable interpolation

* On leave of absence from the Central Research Institute for Physics, Budapest, Hungary.

[1] L. L. Lee, Jr., and J. P. Schiffer, Phys. Rev. Letters **12**, 108 (1964).

[2] L. L. Lee, Jr., and J. P. Schiffer, Phys. Rev. **136**, B405 (1964).

[3] R. Sherr, E. Rost, and M. E. Rickey, Phys. Rev. Letters **12**, 420 (1964).

[4] C. Glashausser and M. E. Rickey, Phys. Rev. **154**, 1033 (1967).

[5] R. C. Johnson and F. D. Santos, Phys. Rev. Letters **19**, 364 (1967).

[6] J. L. Alty, L. L. Green, G. D. Jones, and J. F. Sharpey-Schafer, Nucl. Phys. **100**, 81 (1967).

[7] C. A. Pearson and M. Coz, Nucl. Phys. **82**, 533 (1966); **82**, **545** (1966).

[8] C. A. Pearson and M. Coz, Ann. Phys. (N.Y.) **39**, 199 (1966).

[9] L. Rosen, J. G. Beery, A. S. Goldhaber, and E. H. Auerbach, Ann. Phys. (N.Y.) **34**, 96 (1965).

[10] C. A. Pearson, J. M. Bang, and L. Pocs, Ann. Phys. (N.Y.) (to be published).

[11] C. A. Pearson, J. M. Bang, and L. Pocs, Ann. Phys. (N.Y.) (to be published).